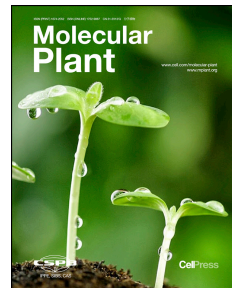


Accepted Manuscript

Clp protease and OR directly control the proteostasis of phytoene synthase, the crucial enzyme for carotenoid biosynthesis in *Arabidopsis*

Ralf Welsch, Xiangjun Zhou, Hui Yuan, Daniel Álvarez, Tianhu Sun, Dennis Schlossarek, Yong Yang, Guoxin Shen, Hong Zhang, Manuel Rodriguez-Concepcion, Theodore W. Thannhauser, Li Li



PII: S1674-2052(17)30336-2
DOI: [10.1016/j.molp.2017.11.003](https://doi.org/10.1016/j.molp.2017.11.003)
Reference: MOLP 545

To appear in: *MOLECULAR PLANT*

Accepted Date: 10 November 2017

Please cite this article as: **Welsch R., Zhou X., Yuan H., Álvarez D., Sun T., Schlossarek D., Yang Y., Shen G., Zhang H., Rodriguez-Concepcion M., Thannhauser T.W., and Li L.** (2017). Clp protease and OR directly control the proteostasis of phytoene synthase, the crucial enzyme for carotenoid biosynthesis in *Arabidopsis*. *Mol. Plant.* doi: 10.1016/j.molp.2017.11.003.

This is a PDF file of an unedited manuscript that has been accepted for publication. As a service to our customers we are providing this early version of the manuscript. The manuscript will undergo copyediting, typesetting, and review of the resulting proof before it is published in its final form. Please note that during the production process errors may be discovered which could affect the content, and all legal disclaimers that apply to the journal pertain.

All studies published in *MOLECULAR PLANT* are embargoed until 3PM ET of the day they are published as corrected proofs on-line. Studies cannot be publicized as accepted manuscripts or uncorrected proofs.

1 **Clp protease and OR directly control the proteostasis of phytoene synthase, the crucial
2 enzyme for carotenoid biosynthesis in Arabidopsis**

3
4 Ralf Welsch^{1,##,*}, Xiangjun Zhou^{2,3,#}, Hui Yuan^{2,3,#}, Daniel Alvarez¹, Tianhu Sun^{2,3}, Dennis
5 Schlossarek¹, Yong Yang², Guoxin Shen⁴, Hong Zhang⁵, Manuel Rodriguez-Concepcion⁶,
6 Theodore W. Thannhauser², and Li Li^{2,3,*}

7
8 ¹ University of Freiburg, Faculty of Biology II, 79104 Freiburg, Germany

9 ² Robert W. Holley Center for Agriculture and Health, USDA-ARS, Cornell University, Ithaca,
10 New York 14853

11 ³ Plant Breeding and Genetics Section, School of Integrative Plant Science, Cornell University,
12 Ithaca, NY 14853

13 ⁴ Zhejiang Academy of Agricultural Sciences, Hangzhou 310021, China

14 ⁵ Department of Biological Sciences, Texas Tech University, Lubbock, TX 79409

15 ⁶ Centre for Research in Agricultural Genomics (CRAG) CSIC-IRTA-UAB-UB, Campus UAB
16 Bellaterra, Barcelona, Spain

17
18 [#] These authors contributed equally to this work

19
20 * Correspondence:

21 Ralf Welsch Li Li

22 Tel: +49-761-203-8454 Tel: +1-607-255-5708

23 E-mail: ralf.welsch@biologie.uni-freiburg.de Email: ll37@cornell.edu

24
25 **Running title:** Post-translational regulation of PSY by Clp protease and OR

26
27 **Short Summary:**

28 We reveal that PSY, the crucial enzyme in the carotenoid biosynthetic pathway, is a substrate of
29 the Clp protease in chloroplasts. The Clp-mediated proteolysis is counteracted by the OR protein
30 to maintain the PSY protein homeostasis and modulate carotenoid biosynthesis in plants. This
31 study demonstrates a new post-translational control mechanism of carotenogenic enzymes.

32

33

34

35 **ABSTRACT**

36

37 Phytoene synthase (PSY) is the crucial plastidial enzyme in the carotenoid biosynthetic pathway.
38 However, its post-translational regulation remains elusive. Likewise, Clp protease constitutes a
39 central part of the plastid protease networks, but its substrates for degradation are not well
40 known. In this study, we report that PSY is a substrate of the Clp protease. PSY was uncovered
41 to physically interact with various Clp protease subunits (*i.e.* ClpS1, ClpC1, and ClpD). High
42 levels of PSY and several other carotenogenic enzymes over-accumulate in the *clpc1*, *clpp4* and
43 *clpr1-2* mutants. The over-accumulated PSY was found to be partially enzymatically active. Loss
44 of the Clp activity in *clpc1* results in reduced rate of PSY protein turnover, further supporting the
45 role of Clp protease in degrading PSY protein. On the other hand, the ORANGE (OR) protein, a
46 major post-translational regulator of PSY with holdase chaperone activity, enhances PSY protein
47 stability and increases the enzymatically active proportion of PSY in *clpc1*, counterbalancing
48 Clp-mediated proteolysis in maintaining PSY protein homeostasis. Collectively, these findings
49 provide novel insights into the quality control of plastid-localized proteins and establish a
50 hitherto unidentified post-translational regulatory mechanism of carotenogenic enzymes in
51 modulating carotenoid biosynthesis in plants.

52

53

54 **Key Words:** carotenoid, phytoene synthase, Clp protease, OR, post-translational regulation,
55 *Arabidopsis*

56

57

58

59

60 **INTRODUCTION**

61
62 Carotenoids play important roles in photosynthesis, photoprotection, phytohormone biosynthesis,
63 and flower/fruit color development (Ruiz-Sola and Rodríguez-Concepción, 2012; Nisar et al.,
64 2015; Yuan et al., 2015a; Sun et al., 2017). Despite great progress in characterizing carotenoid
65 metabolic pathway enzymes, the control mechanisms that maintain carotenogenic enzyme
66 homeostasis are largely unknown.

67
68 Phytoene synthase (PSY) is the crucial enzyme for carotenogenesis and directs carbon flow into
69 the carotenoid biosynthetic pathway (Hirschberg, 1999; Wurtzel et al., 2012). Because of its role
70 in governing carotenoid accumulation, PSY and its regulation have been subjected to intensive
71 investigation (Ruiz-Sola and Rodríguez-Concepción, 2012; Nisar et al., 2015; Yuan et al.,
72 2015a). A number of regulatory genes (i.e. *PIFs*, *HY5*, *RIN*, and *SISGR1*) and factors are known
73 to control *PSY* gene expression (Toledo-Ortiz et al., 2010; Martel et al., 2011; Kachanovsky et
74 al., 2012; Luo et al., 2013; Toledo-Ortiz et al., 2014). However, knowledge of post-translational
75 regulation of PSY remains obscure. Only very recently OR proteins were found to physically
76 interact with PSY and positively regulate its protein abundance and enzymatic activity in plastids
77 (Zhou et al., 2015). PSY translation in *Arabidopsis* was shown to be controlled by differential
78 5'UTR splicing (Alvarez et al., 2016). Further investigation into the regulation of PSY
79 abundance and identification of PSY proteolytic factors are critical to elucidate the delicate
80 mechanisms that control PSY homeostasis for carotenogenesis in plants.

81
82 Intraplastid proteolysis is a key process to maintain protein homeostasis in plastids. The ATP-
83 dependent serine-type Clp protease system constitutes a central part of the plastid protease
84 network. It is critically important for plastids to ensure optimal levels of functional proteins and
85 to remove aggregated, misfolded, or unwanted proteins (Clarke, 2012; Nishimura and van Wijk,
86 2015). Clp protease consists of multiple subunits, which include ClpS as the substrate
87 recognition adaptor, two ClpC (ClpC1-2) and one ClpD subunits as chaperones for substrate
88 unfolding, and five proteolytically active ClpP subunits (ClpP1 and ClpP3 to ClpP6) as well as
89 four proteolytically inactive ClpR subunits (ClpR1 to ClpR4) as core protease components, along
90 with accessory proteins (ClpT1-2) to assembly and stabilize the Clp core (Nishimura and van

91 Wijk, 2015). A plant-specific Clp component ClpF was recently hypothesized to form ClpF-
92 ClpS1 adaptor complex for substrate recognition and delivery (Nishimura et al., 2015).

93
94 Various Clp subunits have been shown to contribute differently to the homeostasis of plastid
95 proteins, such as ClpP1 in the degradation of thylakoid proteins, ClpR1 in the maturation of 23S
96 and 4.5S chloroplast rRNA, and ClpC1 in the turnover of chlorophyllide a oxygenase (Majeran
97 et al., 2000; Koussevitzky et al., 2007; Nakagawara et al., 2007). Recently, ClpC1 was also
98 found to be required for the degradation of deoxyxylulose 5-phosphate synthase (DXS) in the
99 methylerythritol 4-phosphate (MEP) pathway (Pulido et al., 2016). The different Clp subunits
100 also exert distinct functions in affecting plant growth and development (Kim et al., 2009;
101 Moreno et al., 2017). All of the Clp subunits have been identified from both green and non-green
102 plastids in *Arabidopsis* (Peltier et al., 2004; Kim et al., 2009; Olinares et al., 2011). It is obvious
103 that identification of Clp protease targets is critical to understand its involvement and
104 contribution to plastid and plant development. Dozens of chloroplast-localized proteins involved
105 in multiple processes were identified as potential targets of the Clp protease (Nakagawara et al.,
106 2007; Stanne et al., 2009; Nishimura et al., 2013; Nishimura and van Wijk, 2015; Tapken et al.,
107 2015). However, only few proteins were confirmed to be the specific substrates of the Clp
108 protease (Apitz et al., 2016; Pulido et al., 2016). It remains a challenge to identify the specific
109 targets that directly interact with the substrate recognition adaptor ClpS1 and/or the chaperones
110 ClpC and ClpD for degradation (Nishimura and van Wijk, 2015).

111
112 Identification of PSY-interacting proteins is a feasible strategy to explore proteins involved in its
113 post-translational regulation in plastids (Yuan et al., 2015b; Zhou et al., 2015; Chayut et al.,
114 2017). By employing co-immunoprecipitation (co-IP) in conjunction with analysis by mass
115 spectrometry, we identified ClpC1 as a potential PSY-interacting protein. We provide evidence
116 that Clp protease physically interacted with PSY to mediate PSY degradation. By contrast, OR as
117 a major post-translational regulator of PSY promoted its stabilization. Together, Clp protease and
118 OR maintain the homeostasis of PSY in the plastids to assure optimal enzyme protein abundance
119 for adequate carotenoid biosynthesis in plants.

120

121 **RESULTS**

122

123 **Identification of ClpC1 as a Potential PSY-interacting Protein**

124 To discover PSY-interacting proteins, transgenic *Arabidopsis* expressing either *35S:PSY-GFP*
 125 (Supplemental Figure 1) or *35S:GFP* control were generated. Proteins from *35S:PSY-GFP* plants
 126 along with the *35S:GFP* control lines were extracted from four biological replicates and used for
 127 the co-IP experiments. The co-IP products were separated by SDS-PAGE gels and identified by
 128 LC-MS/MS analysis. A total of 202, 235, 238, and 163 proteins were identified from four
 129 biological replicates of co-IPs of *Arabidopsis* expressing PSY-GFP fusion protein, whereas 140,
 130 168, 140 and 122 proteins were found from GFP-only controls in quadruplicates, respectively
 131 (Supplemental Table 1). Among these proteins, 31 were common to the PSY-GFP samples but
 132 absent in the controls (Supplemental Table 2). Interestingly, although the interaction between
 133 PSY and OR was recently demonstrated (Zhou et al., 2015), OR was not co-immunoprecipitated
 134 with PSY as the bait, which may indicate a transient interaction between these two proteins.
 135 Noticeably, geranylgeranyl reductase and a number of plastid chaperone proteins, i.e. HSP70 and
 136 Cpn60, were found as potential PSY-interacting proteins. Interactions between PSY,
 137 geranylgeranyl reductase and geranylgeranyl synthase as well as associations between PSY and
 138 chaperones were reported in previous studies (Bonk et al., 1997; Ruiz-Sola et al., 2016),
 139 indicating viability of the co-IP approach in identification of the potential PSY-interacting
 140 proteins. In the current study, we focused on ClpC1, a key chaperone component of the Clp
 141 protease system (Desimone et al., 1997; Sjögren et al., 2014).

142

143 **PSY Physically Interacts with ClpC1 in Plastids**

144 To confirm the interaction between PSY and ClpC1 inferred from the co-IP results, yeast two-
 145 hybrid (Y2H) analysis was carried out using a split-ubiquitin membrane Y2H system (Obrdlik et
 146 al., 2004). This system has been proved suitable for studying PSY protein interactions (Ruiz-Sola
 147 et al., 2016; Zhou et al., 2015). As shown in Figure 1A, yeast growth on selective medium was
 148 observed when Nub-ClpC1 was mated with PSY-Cub, confirming that PSY physically interacted
 149 with ClpC1 in yeasts. As a negative control, we tested the interaction between ClpC1 and KAT1,
 150 an *Arabidopsis* K⁺ channel protein localized in the plasma membrane (Obrdlik et al., 2004), and
 151 observed no interaction in the Y2H assay (Figure 1A), indicating a specific interaction between
 152 ClpC1 and PSY.

153

154 To further verify PSY and ClpC1 interaction *in vivo*, we performed bimolecular fluorescence
 155 complementation (BiFC) assay. When the N-terminal half of YFP fused to ClpC1 (ClpC1-YN)
 156 and the C-terminal half of YFP fused to PSY (PSY-YC) were co-expressed in tobacco
 157 (*Nicotiana benthamiana*) leaf epidermal cells, YFP signals were observed (Figure 1A). In
 158 contrast, no YFP signals were detected when ClpC1-YN was co-transformed with YC (Figure
 159 1A), or when PSY-YC was with Tic40-YN, a chloroplast inner envelope protein used as negative
 160 control (Supplemental Figure 2A). Such PSY and ClpC1 interaction occurred in chloroplasts,
 161 which is consistent with the plastid localizations of these proteins shown in previous studies
 162 (Desimone et al., 1997; Zhou et al., 2015). The BiFC results confirm direct interaction between
 163 PSY and ClpC1 *in vivo*.

164

165 **PSY also Directly Interacts with Other Clp Protease Subunits Involved in Substrate
 166 Selection**

167 Substrate selection by the Clp protease occurs through the ClpC/D chaperones and adaptor
 168 proteins like ClpS (Clarke, 2012; Nishimura et al., 2015; Nishimura and van Wijk, 2015). To see
 169 whether other Clp protease subunits involved in substrate selection were also physically
 170 associated with PSY, we examined the interactions of PSY with ClpC2, ClpD and ClpS1. By
 171 Y2H assay, we found that ClpD, ClpC2, and ClpS1 all interacted with PSY (Figure 1B). These
 172 PSY-interacting subunits neither interacted with the empty vector control nor with the KAT1
 173 negative control in the Y2H analysis (Figure 1B). To further confirm their interactions *in vivo*,
 174 ClpD and ClpS1 were selected to examine their interactions with PSY in tobacco leaves using
 175 the BiFC assay. Strong YFP signals were observed in chloroplasts when ClpD-YN and ClpS1-
 176 YN were individually co-expressed with PSY-YC in tobacco leaves (Figure 1B). These results
 177 indicate direct interactions between PSY and these Clp protease subunits *in vivo*.

178

179 We also tested our systems with two proteins, PRLI-interacting factor L (pTAC17; AT1G80480)
 180 and ClpF (AT2G03390), which were identified as ClpS1 substrates from affinity-enrichment and
 181 form binary ClpF-ClpS1 adaptor complex (Nishimura et al., 2013; Nishimura et al., 2015).
 182 Interactions with ClpS1 were confirmed by BiFC in tobacco leaves with both proteins,
 183 supporting the suitability of BiFC to study Clp-substrate interactions (Figure 1B). However, both

184 proteins showed strong autoactivation of reporter genes in yeasts, rendering their analysis by
 185 Y2H impossible (see Supplemental Figure 2B).

186

187 In addition, we tested the interaction between PSY and HSP70 (AT5G49910), a protein
 188 identified from the co-IP experiments and known to be involved in folding of DXS (Pulido et al.,
 189 2013; Pulido et al., 2016). PSY was also found to directly interact with HSP70 both in Y2H and
 190 in BiFC assays (Figure 1C).

191

192 **PSY Protein Over-accumulates in *clpc1*, *clpr1-2* and *clpp4***

193 The potential targets of Clp protease likely over-accumulate in various *clp* mutants (Nakagawara
 194 et al., 2007; Stanne et al., 2009; Nishimura and van Wijk, 2015). If PSY were a target of the
 195 chloroplast Clp protease, impairment of the Clp protease activity in the *clp* mutants would be
 196 expected to result in elevated levels of PSY protein. In order to explore this possibility, we
 197 obtained several *clp* mutants from *Arabidopsis* mutant collection (Pulido et al., 2016). As
 198 previously reported (Park and Rodermel, 2004; Sjögren et al., 2004; Kim et al., 2009; Nishimura
 199 et al., 2013), the *clpc1* and *clpr1-2* mutants displayed a pale-green phenotype with smaller
 200 leaves, whereas the *clpc2*, *clpd*, *clps1*, and *clpt1/t2* mutants had no visible phenotype compared
 201 with WT (Figure 2A). In addition, because *clpp4* knockout mutant is embryo-lethal and not
 202 viable (Kim et al., 2013), we generated *clpp4* antisense lines with reduced expression of *ClpP4*
 203 (Supplemental Figure 3B). The *clpp4* antisense lines showed a variegated chlorotic phenotype
 204 (Figure 2A) with small adult plants (Supplemental Figure 3A).

205

206 The PSY protein levels in 3-week-old leaves of these *clp* mutants and WT control were
 207 examined by western blot analysis. In comparison with WT, PSY protein levels were greatly
 208 enhanced in *clpc1*, *clpr1-2* and *clpp4*, but remained similar in the other mutants (Figure 2B).
 209 Quantification of PSY protein levels showed approximately 10-fold increases in the *clpc1*, *clpr1-2*
 210 and *clpp4* mutants compared to the WT control (Figure 2C).

211

212 PSY transcript levels were also measured using real-time RT-PCR. No significant differences
 213 were observed between WT and the *clp* mutant lines (Figure 2D). The result indicates that
 214 deficiency of the Clp subunits in *clpc1*, *clpp4* and *clpr1-2* did not affect PSY transcription. The

215 data also confirms that the observed increase of PSY protein levels in those *clp* mutants was not
 216 a consequence of enhanced gene expression, but occurred post-translationally.

217

218 To rule out that the PSY protein accumulation in *clpc1*, *clpr1-2* and *clpp4* was a consequence of
 219 chloroplast defect, we examined PSY protein levels in some unrelated chlorotic mutants
 220 including *rps5* (Zhang et al., 2016), *xk-1* (Hemmerlin et al., 2006), *toc33* (Jarvis et al., 1998),
 221 *glk1/glk2* (Waters et al., 2008), and *fd2* (Voss et al., 2008). No highly increased PSY protein
 222 levels were observed in these mutants (Figure 2E). The results indicate that the elevated PSY
 223 levels in the *clp* mutants were due to the loss of Clp activity but not chlorosis. In addition, since
 224 PSY was found to directly interact with HSP70-2 (Figure 1C), PSY protein level was also
 225 examined in *hsp70-2*. Interestingly, a slightly elevated PSY protein level was observed in the
 226 *hsp70-2* mutant in comparison with WT control (Figure 2E). The accumulation of PSY in *hsp70-2*
 227 suggests a role of HSP70 in the Clp-mediated PSY homeostasis.

228

229 **PSY Protein Turnover Rate is Reduced in the *clpc1* Mutant**

230 The Clp protease in plastids is responsible for degradation of misfolded or unwanted proteins
 231 (Kato and Sakamoto, 2010; van Wijk, 2015). Various stresses such as heat cause proteins to lose
 232 their native conformation and to form aggregated or misfolded polypeptides (Pulido et al., 2016).

233 To examine whether the Clp protease is responsible for degradation of aggregated or misfolded
 234 PSY, PSY protein turnover rate following heat treatment was monitored in *Arabidopsis* leaves.
 235 Since loss of function of individual Clp complex subunits typically results in decreased
 236 proteolytic activity of the whole complex (Nishimura and van Wijk, 2015) and ClpC1 is the
 237 principle chaperone component of the chloroplast Clp protease (Zheng et al., 2002; Sjögren et
 238 al., 2014), the *clpc1* mutant was used for this study.

239

240 Three-week-old *Arabidopsis* plants of WT and *clpc1* grown at 23 °C were transferred to 42 °C
 241 and rosette leaves were collected at different time points for western blot analysis. As shown in
 242 Figure 3A and 3B, PSY protein level rapidly decreased in the WT control but remained relatively
 243 high in the *clpc1* mutant. At 45 min of treatment, PSY level was reduced to about 30% in the
 244 WT control but maintained at around 70% in *clpc1*. The low PSY degradation rate in *clpc1*

245 indicates a slow proteolytic removal of PSY protein, demonstrating that proper Clp protease
 246 activity was required for maintaining PSY homeostasis.

247

248 **Carotenoid Pathway Activity is Affected in the *clpc1* and *clpr1-2* Mutants**

249 To examine whether carotenoid biosynthesis and accumulation were affected by loss of Clp
 250 protease activity in *Arabidopsis*, we examined pigment formation and carotenoid pathway
 251 activity in the *clp* mutants. Consistent with the mutant plant phenotypes (Figure 2A), chlorophyll
 252 and total carotenoid contents of several *clp* mutants were not significantly different from WT
 253 except *clpc1*, *clpp4* and *clpr1-2*, in which the carotenoid contents were significantly reduced,
 254 especially in *clpp4* with white tissue (Figure 4A and 4B). Interestingly, the immediate product of
 255 PSY, phytoene, was found to accumulate in *clpd*, but absent in WT and all the other *clp* mutants
 256 examined (Figure 4B). Constant ratios of carotenoids to chlorophylls were observed in most
 257 mutants, which mirrored the defined pigment stoichiometry in light-harvesting complex proteins
 258 (Figure 4C).

259

260 With the exception of *clpd*, phytoene usually does not accumulate in leaves and is promptly
 261 metabolized into downstream carotenoids. However, upon treatment with norflurazon (NFZ), an
 262 inhibitor of phytoene desaturase, phytoene accumulates and its level directly reflects PSY
 263 activity and thus carotenoid pathway activity (Rodríguez-Villalón et al., 2009; Lätari et al., 2015;
 264 Zhou et al., 2015). Therefore, we measured the accumulation of phytoene in leaves of 3-week-
 265 old plants treated with NFZ by HPLC (green leaves from *clpp4* were included). In comparison
 266 with the WT control, *clpc1* and *clpr1-2* showed significantly increased phytoene levels whereas
 267 the other *clp* mutants accumulated similar levels of phytoene following NFZ-treatment (Figure
 268 4D). These results suggest that *clpc1* and *clpr1-2* exhibited increased PSY activity, and the
 269 accumulated phytoene in the *clpd* leaves was not caused by increased synthesis. We also
 270 measured the levels of the rest carotenoids and found similar carotenoid accumulation patterns
 271 following NFZ treatment as without NFZ treatment in the *clp* mutants (Supplemental Figure 4).

272

273 **Over-accumulated PSY in *clpc1* and *clpr1-2* is Partially Enzymatically Active**

274 To corroborate the results from carotenoid pathway activity measurements, *in vitro* PSY activity
 275 of *clpc1* and *clpr1-2* along with *clpd* was examined. Active PSY is membrane-associated and

276 usually undetectable in the stromal fractions of chloroplasts in *Arabidopsis* (Welsch et al., 2000;
 277 Lätari et al., 2015), unlike in maize and tomato chromoplasts where soluble PSY1 is
 278 enzymatically active (Fraser et al., 1999; Fraser et al., 2000; Shumskaya et al., 2012). Because
 279 other pathway enzymes compete for the substrate GGPP (*e.g.* chlorophyll biosynthesis),
 280 determination of PSY activity *in vitro* requires separation of stroma and membranes through
 281 plastid fractionation (Welsch et al., 2000; Ruiz-Sola et al., 2016; Zhou et al., 2017).

282

283 The plastid fractionation for PSY activity assay also allowed determination of the enzyme
 284 protein distributions in chloroplast membrane and stromal fractions. While DXS was exclusively
 285 found in the chloroplast stroma in these mutants, the PSY substrate-delivering enzyme GGPS
 286 was present in both stroma and membranes (Figure 5A). Unchanged GGPS protein levels with
 287 similar GGPS activities were observed in the membrane fractions (Figure 5A, Supplemental
 288 Figure 5). In contrast, PSY protein was only detected in the membrane fractions (Figure 5A).
 289 Consistent with the observed PSY over-accumulation in *clpc1* and *clpr1-2* and unchanged PSY
 290 levels in *clpd* (Figure 2B), high levels of PSY protein were noted in *clpc1* and *clpr1-2* in
 291 comparison with WT and *clpd* (Figure 5A).

292

293 In agreement with carotenoid pathway activity measurements in leaves, increased PSY activity
 294 was detected in *clpc1* and *clpr1-2* while *clpd* along with *clpc2* and *clps1* exhibited similar PSY
 295 activity as WT (Figure 5B). Remarkably, the increases in PSY activity and PSY protein levels
 296 were not proportional in the *clpc1* and *clpr1-2* mutants. The specific enzyme activities (*i.e.*
 297 normalized to PSY protein levels) were 53% and 31% lower for *clpc1* and *clpr1-2*, respectively,
 298 than WT (Figure 5C). This indicates that proportions of the over-accumulated PSY were
 299 enzymatically inactive. Immunoblots of chloroplast subfractions confirmed that the inactive
 300 fractions of PSY remained membrane-associated and were not dislocated into the stroma in *clpc1*
 301 and *clpr1-2* (Figure 5A). Moreover, *in vitro* assays also confirmed that the phytoene
 302 accumulation in *clpd* (Figure 4B) was not caused by an increased PSY activity as *clpd* had
 303 similar total and specific PSY activity as WT (Figure 5B-C).

304

305 **Defect in Clp Protease Activity also Results in the Accumulation of Other Carotenogenic
 306 Enzyme Proteins**

307 Recent reports show that *clpc1* and *clpr1-2* contain increased DXS protein levels (Pulido et al.,
 308 2013; Pulido et al., 2016). We analyzed the protein levels of a number of other pathway enzymes
 309 along with DXS in 3-week-old leaves of the *clp* lines. Consistent with recent reports, DXS
 310 protein was found to over-accumulate in *clpc1* and *clpr1-2*. In addition, we observed DXS over-
 311 accumulation in the *clpp4* antisense line (Figure 6). Interestingly, five additional carotenogenic
 312 enzymes, phytoene desaturase (PDS), ζ -carotene desaturase (ZDS), β -carotene hydroxylases
 313 (BCH), carotenoid hydroxylase CYP97A3 (LUT5), and zeaxanthin epoxidase (ZEP), also over-
 314 accumulated in *clpc1*, *clpr1-2* and *clpp4* (Figure 6). The results suggest that several proteins in
 315 the carotenoid biosynthetic pathway could be the targets of Clp proteolysis and that proper Clp
 316 protease activity is required for maintaining proteostasis of these carotenogenic enzymes.

317

318 **OR Delays PSY Degradation**

319 To investigate the post-translational control of PSY that maintains the balance between its
 320 turnover by Clp protease and proper function, we examined the role of OR on PSY protein
 321 stability. Previously, we have shown that OR physically interacts with PSY to positively regulate
 322 PSY protein level and enzyme activity (Zhou et al., 2015). To independently corroborate the
 323 effect of OR on PSY, we constitutively expressed *PSY-GFP* chimeric gene in WT and in *OR*-
 324 overexpression background, and selected lines expressing similar levels of PSY-GFP fusion
 325 protein (Supplemental Figure 6).

326

327 Three-week-old leaf samples were treated with the protein synthesis inhibitor cycloheximide
 328 (CHX). The PSY fusion protein levels in the WT and *OR*-overexpression background were
 329 examined at 3, 6, and 9 h post-treatment by western blot analysis. As shown in Figure 7A, PSY
 330 protein level declined in the *PSY-GFP*/WT leaves, but remained unchanged in the *PSY-GFP*/*OR*
 331 line at 3 h post CHX treatment. PSY fusion protein levels were much higher in the *PSY-GFP*/*OR*
 332 samples than in *PSY-GFP*/WT after CHX treatment at all time points (Figure 7B), showing that
 333 OR was able to stabilize PSY to greatly reduce PSY protein turnover rate.

334

335 **OR Enhances PSY Activity in *clpc1***

336 OR is known to physically interact with PSY and possess holdase activity (Zhou et al., 2015;
 337 Park et al., 2016). To investigate whether OR could promote proper PSY folding to maintain

338 enzymatic activity and counteract PSY degradation by the Clp protease, we introduced OR in a
 339 Clp-defective background by crossing *clpc1* with an *AtOR*-overexpression line (Yuan et al.,
 340 2015b; Zhou et al., 2015). The *clpc1* x *AtOR* F3 plants that were double homozygous for *clpc1*
 341 and the *OR* transgene were generated. Examination of the OR protein levels in the F3 plants
 342 revealed slightly lower OR abundance than in the *AtOR* line used for cross (Figure 7C). *In vivo*
 343 PSY activity was assessed by measuring phytoene accumulation following NFZ treatment in the
 344 3-week-old leaf samples of *clpc1* x *AtOR* plants along with WT, *clpc1*, and the *AtOR*
 345 overexpressor.

346

347 Consistent with the result obtained above, more phytoene was observed in *clpc1* than WT
 348 (Figure 7D). Similarly, more phytoene was detected in the *AtOR* overexpression line than WT as
 349 previously observed (Zhou et al. 2015). However, a higher level of phytoene accumulation was
 350 obtained in the NFZ-treated *clpc1* x *AtOR* line than either in the *AtOR* overexpressor or in *clpc1*
 351 (Figure 7C). The results suggest that OR increased the enzymatically active proportion of PSY in
 352 *clpc1*, possibly through promoting PSY folding or preventing its misfolding/aggregation.

353

354 DISCUSSION

355

356 PSY is a Substrate of Clp Protease

357 PSY catalyzes the critical step in carotenogenesis and directs isoprenoid carbon flow into the
 358 carotenoid biosynthetic pathway (Ruiz-Sola and Rodríguez-Concepción, 2012; Nisar et al., 2015;
 359 Sun et al., 2017). While multiple levels of regulation govern PSY protein amounts and enzymatic
 360 activity, post-translational regulation of PSY including proteolysis of excessive or dysfunctional
 361 PSY protein is important to maintain PSY proteostasis in plastids. In this study, we reveal that
 362 PSY was a substrate of the Clp protease and demonstrate a new post-translational control
 363 mechanism of PSY homeostasis.

364

365 Clp protease is a major protease system in plastids (Clarke, 2012; Nishimura and van Wijk,
 366 2015). The levels of many chloroplast proteins are expected to be controlled by the Clp protease,
 367 but the identities of direct targets of Clp protease remain to be few. Comparative proteomic
 368 analyses of differentially expressed proteins between *Arabidopsis* *clp* mutants and WT identified

369 some upregulated proteins as potential Clp substrates, although many may be due to secondary
370 effects upon loss of the Clp activity (Nishimura et al., 2013; Nishimura and van Wijk, 2015). A
371 recent study confirmed one of these, the first enzyme in 5-aminolevulinic acid biosynthesis
372 glutamyl-tRNA reductase (GluTR), as a direct substrate of the Clp protease (Apitz et al., 2016).
373 Here, we discovered that PSY directly interacted with the adaptor ClpS1 and chaperones ClpC/D
374 (Figure 1). PSY protein levels were greatly increased following the reduction of Clp protease
375 activity in *clpc1*, *clpp4*, and *clpr1-2* (Figure 2). Moreover, the PSY protein degradation rate was
376 reduced when Clp protease was not properly function (Figure 3). These data corroborate PSY as
377 a target of the Clp protease, adding PSY to the substrate list of Clp protease.

378

379 Determination of the substrate selection and delivery mechanisms to proteolyze unwanted
380 proteins in plastids remains a challenge (Nishimura and van Wijk, 2015; van Wijk, 2015). While
381 the selective PSY recognition and delivery mechanisms are currently unclear, data obtained here
382 suggest a number of possible pathways. One is via the ClpS1-ClpF and ClpC1 pathway
383 (Nishimura et al., 2013; Nishimura et al., 2015). In bacteria, adaptor ClpS selects and delivers
384 substrates with an N-terminal degradation signal (an N-degron) for degradation by Clp protease.
385 It is inconclusive whether the N-end rule generally applies to plastid protein proteolysis in plants
386 (Apel et al., 2010; Rowland et al., 2015; Pulido et al., 2016). Here we found that PSY physically
387 interacted with ClpS1. We further examined this interaction by Y2H and found that a 13 amino
388 acid stretch of PSY (PSY71-83) with a putative N-degron interacted with ClpS1 (Supplemental
389 Figure 7). These results suggest a possible role for the ClpS1 adaptor in recognizing and
390 delivering PSY to Clp protease for degradation. However, as PSY protein did not over-
391 accumulate in *clps1*, other adapter(s) or chaperones are likely more crucial and/or used to deliver
392 PSY to the Clp protease.

393

394 A J-protein/Hsp70-dependent pathway for substrate recognition and delivery has been shown
395 recently for DXS (Pulido et al., 2013; Pulido et al., 2016). A J-protein adaptor J20 was found to
396 specifically recognize the inactive forms of DXS and deliver them to Hsp70 chaperones either
397 for proper folding via interaction with ClpB3 (a plastidial Hsp100 chaperone) or for unfolding by
398 ClpC1 for degradation by the Clp protease. We observed a direct interaction between PSY and
399 Hsp70 (Figure 1C), which agrees with the co-existence of PSY and chaperones in high molecular

400 weight complexes in chloroplasts (Bonk et al., 1997). Moreover, we observed slightly elevated
401 PSY protein levels in *hsp70-2* mutant (Figure 2E), suggesting the involvement of Hsp70 in PSY
402 proteostasis. OR is known to directly interact with PSY (Zhou et al., 2015). This raises the
403 question as to whether OR has a J20-analogous function on PSY. However, OR and J20 are
404 different in a number of ways (Pulido et al., 2013; Zhou et al., 2015). In contrast to J20, OR is
405 not a J-protein (Lu et al., 2006). While unfolded DXS protein over-accumulates in *j20*, PSY is
406 almost absent in the *or* mutants. Moreover, *J20* overexpression results in reduced DXS levels
407 while *OR* overexpression increases PSY abundance and activity. Furthermore, no direct
408 interaction was observed between OR and Hsp70 (Supplemental Figure 8). Thus, it is currently
409 unknown as to whether there is a J-protein that specifically recognizes PSY for a J-
410 protein/Hsp70-dependent pathway.

411
412 Our data suggests that the ClpC1-direct pathway might play a key role in selecting and
413 delivering PSY to the Clp core complex. ClpC is the principle chaperone of Clp protease with
414 ClpC1 contributing greatly to substrate unfolding (Sjögren et al., 2014). The ClpC1 chaperone
415 was recently proposed to be more essential in specifically recognizing and directing GluTR1 to
416 the Clp core complex for GluTR1 turnover (Apitz et al., 2016). Here we found that the ClpC1
417 chaperone physically interacted with PSY and was required for PSY degradation by the Clp
418 protease. Lack of ClpC1 resulted in PSY over-accumulation (Figure 2) and slow turnover (Figure
419 3), indicating the important role of ClpC1 for the Clp-mediated PSY degradation.

420
421 Previous studies suggest that the Clp protease controls protein levels of a number of other
422 enzymes required for isoprenoid metabolism. The key enzymes DXS and DXR in the MEP
423 pathway are augmented in the *clp* mutants (Flores-Pérez et al., 2008; Zyballov et al., 2009;
424 Nishimura et al., 2013). Similarly, the MEP pathway enzyme hydroxymethylbutenyl-4-
425 diphosphate synthase (HDS) over-accumulates in the *clp* mutants (Kim et al., 2009; Kim et al.,
426 2013; Kim et al., 2015). Recently, Pulido et al. (2016) showed that the Clp protease plays a
427 primary role for DXS proteolysis. We found that in addition to PSY, carotenogenic enzyme
428 proteins PDS, ZDS, BCH, LUT5 and ZEP also over-accumulated in the *clpc1*, *clpp4* and *clpr1-2*
429 mutants, adding them to the list of potential Clp protease targets. Clearly, a coordinated

430 proteolytic control of both MEP and carotenoid biosynthesis pathways represents an important
 431 mechanism in modulating the steady-state of carotenoids in cells.

432

433 **Both Enzymatically Active and Inactive Forms of PSY Accumulate in *clpc1* and *clpr1-2***

434 Examination of the specific PSY enzyme activities (i.e. normalized to PSY protein levels)
 435 indicates a coexistence of both enzymatically active and inactive PSY forms in *clpc1* and *clpr1-2*
 436 (Figure 5). A large proportion of the over-accumulated PSY protein in the *clp* mutants was
 437 enzymatically inactive, indicating the accumulation of aggregated or misfolded PSY forms.
 438 Previous reports show that PSY is present both as membrane-associated active and stromal non-
 439 active forms (Schledz et al., 1996; Welsch et al., 2000; Lätari et al., 2015). The translocation of
 440 stromal, inactive into membrane-localized, active PSY was observed in de-etiolating seedlings
 441 (Welsch et al., 2000). This probably reflects a developmentally regulated solubilization of PSY,
 442 allowing its re-activation through membrane association during chloroplast formation. Similarly,
 443 a partial stromal relocalization of an inactive PSY population may result from surplus abundance
 444 of PSY through overexpression (Lätari et al., 2015). In both *clpc1* and *clpr1-2*, PSY
 445 quantitatively accumulated in the membrane fractions, thus inactive PSY populations were not
 446 dislocated into the stroma. Apparently, inactive PSY aggregates remain membrane-associated.

447

448 A proportion of the over-accumulated PSY protein in the *clp* mutants was also enzymatically
 449 active, similarly as shown for DXS in *clpc1* (Pulido et al., 2013; Pulido et al., 2016). However, in
 450 contrast to DXS in *clpc1* where the increased DXS correlates with equivalently higher enzymatic
 451 activity (Pulido et al., 2013; Pulido et al., 2016), only about half of the PSY in *clpc1* was
 452 enzymatically active. High DXS activity in *clpc1* was explained by accumulation of chaperones
 453 to prevent DXS aggregation (Pulido et al., 2016). Indeed, we observed an increased level of
 454 Hsp70 in *clpc1* and a few other *clp* mutants (Supplemental Figure 9), and have indications for a
 455 contribution of HSP70-2 to PSY proteostasis (Figure 1C and Figure 2C). However, the major
 456 differences in the proteostatic mechanisms between PSY and DXS might be due to different
 457 localizations. While DXS is soluble in the stroma, PSY requires membrane-association for
 458 activity (Welsch et al., 2000). Membrane integral or associated proteins are known to require a
 459 chaperone-assisted release into membranes upon plastid import (Falk and Sinning, 2010; Liang
 460 et al., 2016). Compared with soluble refolding processes applicable to DXS, proper folding

461 control of membrane proteins poses a particular challenge to protein homeostasis (Liang et al.,
 462 2016). Thus, degradation rather than refolding of misfolded or aggregated PSY might essentially
 463 contribute to PSY proteostasis. Chaperones including OR may help PSY folding to make a
 464 fraction of PSY active in *clpc1*.

465

466 **Carotenoid Patterns in the *clp* Mutants**

467 The overaccumulation of the crucial enzymes for both MEP and carotenoid biosynthetic
 468 pathways disagrees with the reduced pigment content observed in *clpc1* and *clpr1-2* (Figure 4B).
 469 Both DXS and PSY accumulated with higher total activities (Pulido et al., 2016; Figure 5).
 470 Moreover, downstream carotenogenic enzymes like PDS and ZDS also accumulated in *clpc1* and
 471 *clpr1-2* (Figure 6). Desaturation intermediates like phytoene and phytofluene were absent, which
 472 supports unrestricted pathway flow. Therefore, processes other than the synthesis of carotenoids
 473 are likely to account for the reduced carotenoid levels in these *clp* mutants. Clp protease subunits
 474 are known to differentially affect the homeostasis of many plastid proteins (Kim et al., 2009;
 475 Moreno et al., 2017). Defects in ClpC1 and ClpR1-2 affect chloroplast development (Sjögren et
 476 al., 2004; Kim et al., 2009). Since leaf carotenoid contents are determined also by sequestering
 477 structures in addition to biosynthesis, it is possible that the lower levels of carotenoid-binding
 478 proteins (light-harvesting complex proteins) as shown in the *clpc1* mutant (Sjögren et al., 2004)
 479 restrain carotenoid accumulation, leading to reduced carotenoid levels in *clpc1* and *clpr1-2*.

480

481 Surprisingly, in contrast to all other *clp* subunit mutants investigated in this work, leaves of *clpd*
 482 accumulated phytoene (Figure 4B). However, the accumulated phytoene was not due to
 483 increased PSY activity as *in vitro* PSY activity in *clpd* was similar to WT (Figure 5B). Active
 484 PDS requires plastoquinones as electron acceptors, which are reoxidized by the cytochrome-*b*₆*f*-
 485 complex in the photosynthetic electron transport chain with a contribution of the plastid terminal
 486 oxidase (McDonald et al., 2011). Accordingly, mutants with impaired biosynthesis or
 487 reoxidation of plastoquinones accumulate phytoene in their leaves (Norris et al., 1995; Carol et
 488 al., 1999). Thus, it is possible that a defective ClpD impacted protein(s) associated with
 489 plastoquinone biosynthesis or regeneration to affect phytoene desaturation, resulting in the
 490 accumulation of phytoene in *clpd*.

491

492 **OR and Clp Protease Counterbalance PSY Activity and Degradation**

493 Our previous studies show that OR physically interacts with PSY to positively regulate PSY
 494 protein level and enzyme activity (Zhou et al., 2015; Chayut et al., 2017). OR appears to perform
 495 this function by maintaining PSY in a properly folded form and preventing PSY degradation by
 496 the Clp protease. This is supported by our experiments demonstrating an increased PSY protein
 497 stability in the *OR* overexpression background and enhanced PSY activity in the *clpc1 x AtOR*
 498 line (Figure 7). It is also supported by the recent discovery that OR possesses holdase activity to
 499 prevent PSY misfolding and aggregation (Park et al., 2016). Moreover, PSY is barely present in
 500 the *ator ator-like* double mutant and in the melon fruits of *lowβ* mutant (Zhou et al., 2015;
 501 Chayut et al., 2017), which results from lack of OR to protect PSY thus enhancing its
 502 degradation.

503

504 Based on the data obtained, we propose a model for Clp protease and OR in governing the
 505 balance between PSY turnover and activity in plastids (Figure 8). OR as a membrane protein
 506 physically interacts with PSY for membranes-association in its active form for carotenogenesis.
 507 Inactive misfolded and/or aggregated forms of PSY are likely recognized by ClpC1, either
 508 directly or upon recognition and delivery by ClpS1, and unfolded prior to proteolysis by the core
 509 Clp protease components. Upon increased OR abundance in the *AtOR*-overexpressing tissues,
 510 PSY protein is maintained in an active, membrane-associated state and thus prevented from
 511 proteolysis, while absence of OR results in PSY degradation, a regulation that occurs solely
 512 posttranslational. The suggested regulatory mechanism shares similarities with the
 513 posttranslational regulation of tetrapyrrole and thus chlorophyll biosynthesis, catalyzed by
 514 GluTR (Apitz et al., 2016). The similar posttranslational regulations of crucial enzymes for the
 515 synthesis of major photosynthetic pigments, GluTR for tetrapyrrole and PSY for carotenoid
 516 biosynthesis, might contribute to an efficient coordinated supply of stoichiometrically balanced
 517 amounts for accurate assembly of photosynthetic complexes in chloroplasts.

518

519 **METHODS**

520

521 **Plant Materials**

522 *Arabidopsis thaliana* WT (ecotype Columbia-0) and mutant lines as well as *Nicotiana*
523 *benthamiana* plants used for transformation were grown in soil under 14 h light/10 h dark at 23
524 °C. The T-DNA insertion mutant lines used here included *clps1*, *clpc1*, *clpc2*, *clpd*, *clpr1-2*, and
525 *clpt1/t2* (Pulido et al., 2016). The *clpp4* antisense line was generated by introducing *ClpP4*
526 antisense construct into *Arabidopsis* (ecotype Columbia-0). The *clpc1* was also crossed with an
527 *AtOR* overexpressor (Zhou et al., 2015; Yuan et al., 2015b) to produce *clpcl* x *AtOR* homozygous
528 line. The *PSY-GFP* transgenic lines in WT and *OR* expressing backgrounds were produced by
529 introducing 35S:*PSY-GFP* construct into *Arabidopsis* WT and the *OR*-overexpressing transgenic
530 plants. The *rps5*, *xk-1*, *glk1/glk2*, *toc33*, *fd2*, and *hsp70-2* mutants were either ordered from
531 ABRC or obtained from collaborators.

532

533 **Co-Immunoprecipitation (Co-IP)**

534 Co-immunoprecipitation was conducted with quadruplicate biological replicates as described
535 previously (Zhou et al., 2015). Briefly, proteins were extracted from *Arabidopsis* plants
536 expressing 35S:*PSY-GFP* or 35S:*GFP*, mixed with magnetic beads conjugated to anti-GFP
537 antibodies (Miltenyi Biotec Inc. Auburn, CA), and incubated on ice for 30 min. Protein
538 complexes containing PSY-GFP and GFP were purified in μ columns by washing 4 times with
539 extraction buffer and eluting with 2 x SDS loading buffer.

540

541 **Proteomics analysis**

542 The immunoprecipitated proteins were resolved on SDS-PAGE gels and then excised into 10
543 bands that were subjected to subsequent in-gel digestion as detailed previously (Yang et al.,
544 2007). The digests were analyzed using a nanoACQUITY UPLC™ system coupled with a
545 Synapt HDMSTM (Waters) mass spectrometer (MS) equipped with a NanoLockSpray source
546 (Wang et al., 2013). All of the raw data were output as PKL files by the ProteinLynx Global
547 Server 2.4 (PLGS, Waters). Subsequent database searches were carried out by Mascot Daemon
548 2.3 (Matrix Science, Boston, MA) against *Arabidopsis* databases (Araport11_latest
549 <https://www.araport.org/>). The search parameters used for the Mascot analysis were: one missed
550 cleavage site by trypsin allowed with fixed carbamidomethyl modification of cysteine, and
551 variable of oxidation on methionine and deamidation of Asn and Gln residues. The peptide and
552 fragment mass tolerance values were 15 ppm and 0.1 Da, respectively. To reduce the probability

553 of false identification, only peptides with significance scores at the 99% confidence interval were
 554 counted as identified (Wang et al., 2013).

555

556 **Yeast Two-Hybrid Assay**

557 The split ubiquitin system was used as described previously (Zhou et al., 2015). The cDNA
 558 sequences of *ClpC1* (At5g50920), *ClpC2* (At3g48870), *ClpD* (At5g51070), and *ClpS1*
 559 (At1g68660) along with plastidial Hsp70-2 (At5g49910) without the sequences encoding their
 560 transit peptides were cloned to make Nub plasmids. The cDNA sequence of an *Arabidopsis* K⁺
 561 channel subunit *KAT* (At5g46240; Obrdlik et al., 2004) used as negative control was cloned into
 562 the Cub expressing vector. The PSY-Cub and OR-Cub vectors were from the previous study
 563 (Zhou et al., 2015). Plasmids were transformed into yeast strain THY.AP4 (Nub) or THY.AP5
 564 (Cub) and mated with each other. Interactions were examined by placing yeast strains with a
 565 series of dilutions on selection medium lacking leucine, tryptophan, adenine and histidine (-
 566 LWAH) with 300 μM methionine supplementation after 2 days of growth at 29°C.

567

568 **Bimolecular Fluorescence Complementation (BiFC) Assay**

569 The *ClpC1*, *ClpD*, and *ClpS1* as well as *HSP70-2*, *TAC17* (At1g80480) and *ClpF* (At2g03390)
 570 coding regions without stop codons were individually cloned into pSPYNE173 vector (Waadt et
 571 al., 2008) between the appropriate restriction enzyme sites, and then transferred into *A.*
 572 *tumefaciens* strain GV3101. *Agrobacterium* cells carrying the PSY and individual *Clp* constructs
 573 were infiltrated into 4-week-old *N. benthamiana* leaves as previously described (Zhou et al.,
 574 2015). Two days after infiltration, YFP fluorescence was detected using a Leica TCS SP5 Laser
 575 Scanning Confocal Microscope (Leica Microsystems, Exon, PA USA) with excitation
 576 wavelength at 488 nm and emission filter at 520 nm. Chloroplasts were excited with the blue
 577 argon laser (488 nm), and emitted light was collected at 680 nm to 700 nm.

578

579 **Immunoblotting Analysis**

580 Total proteins were extracted from *Arabidopsis* leaves using the phenol method as described
 581 (Wang et al., 2013). Proteins were resolved on SDS-PAGE gels, transferred onto nitrocellulose
 582 membranes (B85), and blocked with TBS buffer containing 5% milk for 1 hr at room
 583 temperature. Membranes were incubated with antibodies against GGPS11 (Eurogentec,

584 Belgium), PSY (Abmart, Shanghai, China), DXS (Philippe Hugueney, INRA, France), PDS (Al-
 585 Bibili et al., 1996), ZDS (Eurogentec, Belgium), BCH (Abmart, Shanghai, China), ZEP
 586 (Agrisera), OR (Lu et al., 2006), or actin (Sigma) in TBS buffer containing 1% milk for 2 h. The
 587 ECL reagent (GE Healthcare, München, Germany) was used as the detection system. The
 588 relative protein levels were quantified using ImageJ (Schneider et al., 2012).

589

590 **Phytoene Synthase Degradation and Stability Assays**

591 To examine the effect of Clp protease on PSY degradation, 3-week-old *Arabidopsis* plants of
 592 WT and *clpC1* grown at 23 °C were transferred to 42 °C for heat shock treatment and rosette
 593 leaves were collected at different times after treatment. To measure the PSY stability, 3-week-
 594 old rosette leaf discs of PSY-GFP lines in the *Arabidopsis* WT and *OR* overexpressor
 595 backgrounds were treated with 100 µM cycloheximide (CHX) for various times. Total proteins
 596 from treated samples were extracted and immunoblot-analyzed (Zhou et al., 2015). Protein
 597 concentrations were determined by the Bradford method. The PSY protein was immunoblotted
 598 with anti-PSY antibody for PSY degradation assay and with anti-GFP for stability assay.

599

600 **Chloroplast Isolation and *In vitro* Enzyme Activity Assays**

601 *In vitro* PSY activity assay was carried with isolated chloroplast membranes as described (Zhou
 602 et al., 2015). Briefly, chloroplasts were isolated from leaves of three-week old plants, and lysed
 603 as described (van Wijk et al., 2007). Protein amounts were determined by Bradford assay (Bio-
 604 Rad). Plastid membranes (100 µg protein) were incubated in a reaction mixture containing [¹⁴C]-
 605 isopentenyl diphosphate (IPP, 50 mCi mmol⁻¹; American Radiolabeled Chemicals), IPP,
 606 dimethylallyl diphosphate (DMAPP), and 10 µg purified *Arabidopsis* GGPPS11. Radioactive
 607 labelled products were analyzed and quantified as described (Welsch et al., 2000). [¹⁴C]-GGPP
 608 and [¹⁴C]-phytoene synthesis occurred linearly within the first 45 min after substrate addition.
 609 PSY activities in different samples were determined after 15 min incubation. Stromal proteins
 610 were concentrated by ultrafiltration (Microcon, MWCO 3 kD, Millipore).

611

612 **RNA Extraction, Reverse Transcription and Quantitative RT-PCR**

613 Total RNA was extracted from *Arabidopsis* leaves using TRIzol reagent according to the
 614 manufacturer's instruction (Life Technologies, Carlsbad, CA). cDNA was synthesized using

615 SuperScript™ III Reverse Transcriptase (Invitrogen, Carlsbad, CA) after RQ1 DNase treatment.
616 Quantitative RT-PCR was performed using SYBR master mix (Bio-Rad, Hercules, CA) with
617 gene specific primers (Supplemental Table 3) as described (Zhou et al., 2011a). The relative
618 expression of selected genes was normalized to an *Arabidopsis actin* gene.

619

620 **Pigment Analysis**

621 Total carotenoid and chlorophyll extraction and HPLC analysis of carotenoids were performed as
622 described (Welsch et al., 2008). Chlorophylls were extracted with 80% acetone and determined
623 as previously described (Zhou et al., 2011b). Norflurazon (NFZ) treatments were done according
624 to Zhou et al. (2015). Leaves from three-week old plants were detached, immediately transferred
625 onto 70 mM NFZ and incubated for two hours in the dark. Leaves were transferred onto 10 mM
626 NFZ and further incubated for four hours with 100 μmol photons $\text{m}^{-2}\text{s}^{-1}$. Leaves were incubated
627 with the adaxial surface facing the air. Leaves were harvested immediately, frozen in liquid
628 nitrogen, and lyophilized before carotenoid extraction.

629

630 **AUTHOR CONTRIBUTIONS**

631 RW, XZ, HY, DA, TS, DS, and YY performed the experiments and data analysis. RW, XZ, HY,
632 and LL designed the research. TT guided the proteomics experiments and data analysis. GS, HZ,
633 and MRC provided research agents. MRC assisted in data analysis and interpretation. RW, XZ,
634 and LL wrote the manuscript. All authors contributed to the final manuscript.

635

636 **ACKNOWLEDGEMENTS**

637 We are grateful to Dr. Klaas van Wijk (Cornell University) for his critical comments and helpful
638 suggestions to improve this paper. We thank Dr. Hongbin Zhang for performing the BiFC
639 experiments between ClpS1 and TAC/ClpF, Ms. Caroline Rodriguez, Sarah Melesse (Cornell
640 University) and Carmen Schubert (University of Freiburg) for technical assistance. We thank Dr.
641 Julian Koschmieder (University of Freiburg) for supplying antibodies against PDS and ZDS, Dr.
642 Philippe Hugueney (Université de Strasbourg, France) for anti-DXS antibodies and Dr. Roberto
643 Bassi (Università di Verona, Italy) for antibodies against LUT5. This work was supported by
644 Agriculture and Food Research Initiative competitive award no. 2016-67013-24612 from the

645 USDA National Institute of Food and Agriculture and by the HarvestPlus research consortium.
 646 The authors declare no conflict of interest.

647

648

649 **REFERENCES**

650 **Al-Babili, S., von Lintig, J., Haubruck, H., and Beyer, P.** (1996). A novel, soluble form of
 651 phytoene desaturase from *Narcissus pseudonarcissus* chromoplasts is Hsp70-complexed and
 652 competent for flavinylation, membrane association and enzymatic activation. *Plant J.* **9**, 601-
 653 612.

654 **Alvarez, D., Voß, B., Maass, D., Wüst, F., Schaub, P., Beyer, P., and Welsch, R.** (2016).
 655 Carotenogenesis is regulated by 5'UTR-mediated translation of phytoene synthase splice
 656 variants. *Plant Physiol.* **172**, 2314-2326.

657 **Apel, W., Schulze, W.X., and Bock, R.** (2010). Identification of protein stability determinants in
 658 chloroplasts. *Plant J.* **63**, 636-650.

659 **Apitz, J., Nishimura, K., Schmied, J., Wolf, A., Hedtke, B., van Wijk, K.J., and Grimm, B.**
 660 (2016). Posttranslational control of ALA synthesis includes GluTR degradation by Clp
 661 protease and stabilization by GluTR-binding protein. *Plant Physiol.* **170**, 2040-2051.

662 **Bonk, M., Hoffmann, B., Von Lintig, J., Schledz, M., Al-Babili, S., Hobeika, E., Kleinig, H.,**
 663 **and Beyer, P.** (1997). Chloroplast import of four carotenoid biosynthetic enzymes in vitro
 664 reveals differential fates prior to membrane binding and oligomeric assembly. *Eur. J.*
 665 *Biochem.* **247**, 942-950.

666 **Carol, P., Stevenson, D., Bisanz, C., Breitenbach, J., Sandmann, G., Mache, R., Coupland,**
 667 **G., Kuntz, M.** (1999). Mutations in the *Arabidopsis* gene *IMMUTANS* cause a variegated
 668 phenotype by inactivating a chloroplast terminal oxidase associated with phytoene
 669 desaturation. *Plant Cell* **11**, 57-68.

670 **Chayut, N., Yuan, H., Ohali, S., Meir, A., Sa'ar, U., Tzuri, G., Zheng, Y., Mazourek, M.,**
 671 **Gepstein, S., Zhou, X., Portnoy, V., Lewinsohn, E., Schaffer, A.A., Katzir, N., Fei, Z.,**
 672 **Welsch, R., Li, L., Burger, J., and Tadmor, Y.** (2017). Distinct mechanisms of the
 673 ORANGE protein in controlling carotenoid flux. *Plant Physiol.* **173**, 376-389.

674 **Clarke, A.K.** (2012). The chloroplast ATP-dependent Clp protease in vascular plants - new
 675 dimensions and future challenges. *Physiol. Plant* **145**, 235-244.

676 **Desimone, M., Weiß-Wichert, C., Wagner, E., Altenfeld, U., Johanningmeier, U.** **1997.**
 677 Immunochemical Studies on the Clp-protease in Chloroplasts: Evidence for the Formation of
 678 a ClpC/P Complex. *Bot Acta* **110**, 234-239.

679 **Falk, S., and Sinning, I.** (2010). cpSRP43 is a novel chaperone specific for light-harvesting
 680 chlorophyll a,b-binding proteins. *J. Biol. Chem.* **285**, 21655-21661.

681 **Fraser, P.D., Kiano, J.W., Truesdale, M.R., Schuch, W., Bramley, P.M. (1999).** Phytoene
 682 synthase-2 enzyme activity in tomato does not contribute to carotenoid synthesis in ripening
 683 fruit. *Plant Mol. Biol.* **40**, 687–698.

684 **Fraser, P.D., Schuch, W., Bramley, P.M. (2000).** Phytoene synthase from tomato (*Lycopersicon*
 685 *esculentum*) chloroplasts--partial purification and biochemical properties. *Planta* **211**, 361–
 686 369.

687 **Flores-Pérez, U., Sauret-Güeto, S., Gas, E., Jarvis, P., and Rodríguez-Concepción, M.**
 688 (2008). A mutant impaired in the production of plastome-encoded proteins uncovers a
 689 mechanism for the homeostasis of isoprenoid biosynthetic enzymes in *Arabidopsis* plastids.
 690 *Plant Cell* **20**, 1303-1315.

691 **Hemmerlin, A., Tritsch, D., Hartmann, M., Pacaud, K., Hoeffler, J.F., van Dorsselaer, A.,**
 692 **Rohmer, M., and Bach, T.J. (2006).** A cytosolic *Arabidopsis* D-xylulose kinase catalyzes
 693 the phosphorylation of 1-deoxy-D-xylulose into a precursor of the plastidial isoprenoid
 694 pathway. *Plant Physiol* **142**, 441-457.

695 **Hirschberg, J. (1999).** Production of high-value compounds: carotenoids and vitamin E. *Curr.*
 696 *Opin. Biotechnol.* **10**, 186-191.

697 **Jarvis, P., Chen, L.J., Li, H., Peto, C.A., Fankhauser, C., and Chory, J. (1998).** An
 698 *Arabidopsis* mutant defective in the plastid general protein import apparatus. *Science* **282**,
 699 100-103.

700 **Kachanovsky, D.E., Filler, S., Isaacson, T., and Hirschberg, J. (2012).** Epistasis in tomato
 701 color mutations involves regulation of *phytoene synthase 1* expression by *cis*-carotenoids.
 702 *Proc. Natl. Acad. Sci. USA* **109**, 19021-19026.

703 **Kato, Y., and Sakamoto, W. (2010).** New insights into the types and function of proteases in
 704 plastids. *Int. Rev. Cell Mol. Biol.* **280**, 185-218.

705 **Kim, J., Rudella, A., Ramirez Rodriguez, V., Zyballov, B., Olinares, P.D., and van Wijk, K.J.**
 706 (2009). Subunits of the plastid ClpPR protease complex have differential contributions to
 707 embryogenesis, plastid biogenesis, and plant development in *Arabidopsis*. *Plant Cell* **21**,
 708 1669-1692.

709 **Kim, J., Olinares, P.D., Oh, S.H., Ghisaura, S., Poliakov, A., Ponnala, L., and van Wijk, K.J.**
 710 (2013). Modified Clp protease complex in the ClpP3 null mutant and consequences for
 711 chloroplast development and function in *Arabidopsis*. *Plant Physiol.* **162**, 157-179.

712 **Kim, J., Kimber, M.S., Nishimura, K., Friso, G., Schultz, L., Ponnala, L., and van Wijk, K.J.**
 713 (2015). Structures, functions, and interactions of ClpT1 and ClpT2 in the Clp protease
 714 system of *Arabidopsis* chloroplasts. *Plant Cell* **27**, 1477-1496.

715 **Koussevitzky, S., Stanne, T.M., Peto, C.A., Giap, T., Sjögren, L.L., Zhao, Y., Clarke, A.K.,**
 716 **and Chory, J. (2007).** An *Arabidopsis thaliana* virescent mutant reveals a role for ClpR1 in
 717 plastid development. *Plant Mol. Biol.* **63**, 85-96.

718 **Liang, F.C., Kroon, G., McAvoy, C.Z., Chi, C., Wright, P.E., and Shan, S.O.** (2016).
 719 Conformational dynamics of a membrane protein chaperone enables spatially regulated
 720 substrate capture and release. *Proc. Natl. Acad. Sci. USA* **113**, E1615-1624.

721 **Lu, S., Van Eck, J., Zhou, X., Lopez, A.B., O'Halloran, D.M., Cosman, K.M., Conlin, B.J.,**

722 **Paolillo, D.J., Garvin, D.F., Vrebalov, J., Kochian, L.V., Küpper, H., Earle, E.D., Cao, J.,**

723 **and Li, L.** (2006). The cauliflower *Or* gene encodes a DnaJ cysteine-rich domain-containing
 724 protein that mediates high levels of beta-carotene accumulation. *Plant Cell* **18**, 3594-3605.

725 **Luo, Z., Zhang, J., Li, J., Yang, C., Wang, T., Ouyang, B., Li, H., Giovannoni, J., and Ye, Z.**
 726 (2013). A STAY-GREEN protein SISGR1 regulates lycopene and β -carotene accumulation
 727 by interacting directly with SIPSY1 during ripening processes in tomato. *New Phytol.* **198**,
 728 442-452.

729 **Lätari, K., Wüst, F., Hübner, M., Schaub, P., Beisel, K.G., Matsubara, S., Beyer, P., and**

730 **Welsch, R.** (2015). Tissue-specific apocarotenoid glycosylation contributes to carotenoid
 731 homeostasis in *Arabidopsis* leaves. *Plant Physiol.* **168**, 1550-1562.

732 **McDonald, A.E., Ivanov, A.G., Bode, R., Maxwell, D.P., Rodermel, S.R., and Hüner, N.P.**
 733 (2011). Flexibility in photosynthetic electron transport: the physiological role of plastoquinol
 734 terminal oxidase (PTOX). *Biochim. Biophys. Acta* **1807**, 954-967. **Majeran, W., Wollman,**
 735 **F.A., and Vallon, O.** (2000). Evidence for a role of ClpP in the degradation of the
 736 chloroplast cytochrome *b*₆*f* complex. *Plant Cell* **12**, 137-150.

737 **Martel, C., Vrebalov, J., Tafelmeyer, P., and Giovannoni, J.J.** (2011). The tomato MADS-box
 738 transcription factor RIPENING INHIBITOR interacts with promoters involved in numerous
 739 ripening processes in a COLORLESS NONRIPENING-dependent manner. *Plant Physiol.*
 740 **157**, 1568-1579.

741 **Moreno, J.C., Tiller, N., Diez, M., Karcher, D., Tillich, M., Schöttler, M.A., and Bock, R.**
 742 (2017). Generation and characterization of a collection of knock-down lines for the
 743 chloroplast Clp protease complex in tobacco. *J. Exp. Bot.* **68**, 2199-2218.

744 **Nakagawara, E., Sakuraba, Y., Yamasato, A., Tanaka, R., and Tanaka, A.** (2007). Clp
 745 protease controls chlorophyll b synthesis by regulating the level of chlorophyllide a
 746 oxygenase. *Plant J.* **49**, 800-809.

747 **Nisar, N., Li, L., Lu, S., Khin, N.C., and Pogson, B.J.** (2015). Carotenoid metabolism in plants.
 748 *Mol. Plant* **8**, 68-82.

749 **Nishimura, K., and van Wijk, K.J.** (2015). Organization, function and substrates of the
 750 essential Clp protease system in plastids. *Biochim. Biophys. Acta* **1847**, 915-930.

751 **Nishimura, K., Apitz, J., Friso, G., Kim, J., Ponnala, L., Grimm, B., and van Wijk, K.J.**
 752 (2015). Discovery of a unique Clp component, ClpF, in chloroplasts: a proposed binary
 753 ClpF-ClpS1 adaptor complex functions in substrate recognition and delivery. *Plant Cell* **27**,
 754 2677-2691.

755 **Nishimura, K., Asakura, Y., Friso, G., Kim, J., Oh, S.H., Rutschow, H., Ponnala, L., and**
 756 **van Wijk, K.J.** (2013). ClpS1 is a conserved substrate selector for the chloroplast Clp
 757 protease system in *Arabidopsis*. *Plant Cell* **25**, 2276-2301.

758 **Norris, S.R., Barrette, T.R., and DellaPenna, D.** (1995). Genetic dissection of carotenoid
 759 synthesis in *Arabidopsis* defines plastoquinone as an essential component of phytoene
 760 desaturation. *Plant Cell* **7**, 2139-2149.

761 **Obregon, P., El-Bakkoury, M., Hamacher, T., Cappellaro, C., Vilarino, C., Fleischer, C.,**
 762 **Ellerbrok, H., Kamuzinzi, R., Ledent, V., Blaudez, D., Sanders, D., Revuelta, J.L., Boles,**
 763 **E., Andre, B., and Frommer, W.B.** (2004). K⁺ channel interactions detected by a genetic
 764 system optimized for systematic studies of membrane protein interactions. *K+* channel
 765 interactions detected by a genetic system optimized for systematic studies of membrane
 766 protein interactions. *Proc. Natl. Acad. Sci. USA* **101**, 12242-12247.

767 **Olinares, P.D., Kim, J., and van Wijk, K.J.** (2011). The Clp protease system; a central
 768 component of the chloroplast protease network. *Biochim. Biophys. Acta* **1807**, 999-1011.

769 **Park, S., and Rodermel, S.R.** (2004). Mutations in ClpC2/Hsp100 suppress the requirement for
 770 FtsH in thylakoid membrane biogenesis. *Proc. Natl. Acad. Sci. USA* **101**, 12765-12770.

771 **Park, S., Kim, H.S., Jung, Y.J., Kim, S.H., Ji, C.Y., Wang, Z., Jeong, J.C., Lee, H.S., Lee,**
 772 **S.Y., and Kwak, S.S.** (2016). Orange protein has a role in phytoene synthase stabilization in
 773 sweetpotato. *Sci. Rep.* **6**, 33563.

774 **Peltier, J.B., Ripoll, D.R., Friso, G., Rudella, A., Cai, Y., Ytterberg, J., Giacomelli, L.,**
 775 **Pillard, J., and van Wijk, K.J.** (2004). Clp protease complexes from photosynthetic and
 776 non-photosynthetic plastids and mitochondria of plants, their predicted three-dimensional
 777 structures, and functional implications. *J. Biol. Chem.* **279**, 4768-4781.

778 **Pulido, P., Toledo-Ortiz, G., Phillips, M.A., Wright, L.P., and Rodríguez-Concepción, M.**
 779 (2013). *Arabidopsis* J-protein J20 delivers the first enzyme of the plastidial isoprenoid
 780 pathway to protein quality control. *Plant Cell* **25**, 4183-4194.

781 **Pulido, P., Llamas, E., Llorente, B., Ventura, S., Wright, L.P., and Rodríguez-Concepción, M.**
 782 (2016). Specific Hsp100 chaperones determine the fate of the first enzyme of the
 783 plastidial isoprenoid pathway for either refolding or degradation by the stromal Clp protease
 784 in *Arabidopsis*. *PLoS Genet.* **12**, e1005824.

785 **Rodríguez-Villalón, A., Gas, E., and Rodríguez-Concepción, M.** (2009). Phytoene synthase
 786 activity controls the biosynthesis of carotenoids and the supply of their metabolic precursors
 787 in dark-grown *Arabidopsis* seedlings. *Plant J.* **60**, 424-435.

788 **Rowland, E., Kim, J., Bhuiyan, N.H., and van Wijk, K.J.** (2015). The *Arabidopsis* chloroplast
 789 stromal N-terminome: complexities of amino-terminal protein maturation and stability. *Plant*
 790 *Physiol.* **169**, 1881-1896.

791 **Ruiz-Sola, M., and Rodríguez-Concepción, M.** (2012). Carotenoid biosynthesis in *Arabidopsis*:

792 a colorful pathway. *Arabidopsis Book* **10**, e0158.

793 **Ruiz-Sola, M., Coman, D., Beck, G., Barja, M.V., Colinas, M., Graf, A., Welsch, R.,**
 794 **Rütimann, P., Bühlmann, P., Bigler, L., Grussem, W., Rodríguez-Concepción, M., and**
 795 **Vranová, E.** (2016). *Arabidopsis* GERANYLGERANYL DIPHOSPHATE SYNTHASE 11
 796 is a hub isozyme required for the production of most photosynthesis-related isoprenoids.
 797 *New Phytol.* **209**, 252-264.

798 **Schledz, M., al-Babili, S., von Lintig, J., Haubruck, H., Rabbani, S., Kleinig, H., and Beyer,**
 799 **P.** (1996). Phytoene synthase from *Narcissus pseudonarcissus*: functional expression,
 800 galactolipid requirement, topological distribution in chromoplasts and induction during
 801 flowering. *Plant J.* **10**, 781-792.

802 **Schneider, C.A., Rasband, W.S., and Eliceiri, K.W.** (2012). NIH Image to ImageJ: 25 years of
 803 image analysis. *Nat. Meth.* **9**, 671-675.

804 **Shumskaya, M., Bradbury, L.M.T., Monaco, R.R., Wurtzel, E.T.** (2012). Plastid localization
 805 of the key carotenoid enzyme phytoene synthase is altered by isozyme, allelic variation, and
 806 activity. *Plant Cell* **24**, 3725-3741.

807 **Sjögren, L.L., MacDonald, T.M., Sutinen, S., and Clarke, A.K.** (2004). Inactivation of the
 808 *clpC1* gene encoding a chloroplast Hsp100 molecular chaperone causes growth retardation,
 809 leaf chlorosis, lower photosynthetic activity, and a specific reduction in photosystem content.
 810 *Plant Physiol.* **136**, 4114-4126.

811 **Sjögren, L.L., Tanabe, N., Lymeropoulos, P., Khan, N.Z., Rodermel, S.R., Aronsson, H.,**
 812 **and Clarke, A.K.** (2014). Quantitative analysis of the chloroplast molecular chaperone
 813 ClpC/Hsp93 in *Arabidopsis* reveals new insights into its localization, interaction with the
 814 Clp proteolytic core, and functional importance. *J. Biol. Chem.* **289**, 11318-11330.

815 **Stanne, T.M., Sjögren, L.L., Koussevitzky, S., and Clarke, A.K.** (2009). Identification of new
 816 protein substrates for the chloroplast ATP-dependent Clp protease supports its constitutive
 817 role in *Arabidopsis*. *Biochem. J.* **417**, 257-268.

818 **Sun, T., Yuan, H., Cao, H., Yazdani, M., Tadmor, Y., Li, L.** (2017). Carotenoid metabolism in
 819 plants: The role of plastids. *Mol. Plant* doi: 10.1016/j.molp.2017.09.010.

820 **Tapken, W., Kim, J., Nishimura, K., van Wijk, K.J., and Pilon, M.** (2015). The Clp protease
 821 system is required for copper ion-dependent turnover of the PAA2/HMA8 copper transporter
 822 in chloroplasts. *New Phytol.* **205**, 511-517.

823 **Toledo-Ortiz, G., Huq, E., and Rodríguez-Concepción, M.** (2010). Direct regulation of
 824 phytoene synthase gene expression and carotenoid biosynthesis by phytochrome-interacting
 825 factors. *Proc. Natl. Acad. Sci. USA* **107**, 11626-11631.

826 **Toledo-Ortiz, G., Johansson, H., Lee, K.P., Bou-Torrent, J., Stewart, K., Steel, G.,**
 827 **Rodríguez-Concepción, M., and Halliday, K.J.** (2014). The HY5-PIF regulatory module
 828 coordinates light and temperature control of photosynthetic gene transcription. *PLoS Genet.*

829 **10**, e1004416.

830 **van Wijk, K.J.** (2015). Protein maturation and proteolysis in plant plastids, mitochondria, and
831 peroxisomes. *Annu. Rev. Plant Biol.* **66**, 75-111.

832 **van Wijk, K.J., Peltier, J.B., and Giacomelli, L.** (2007). Isolation of chloroplast proteins from
833 *Arabidopsis thaliana* for proteome analysis. *Methods Mol. Biol.* **355**, 43-48.

834 **Voss, I., Koelmann, M., Wojtera, J., Holtgrefe, S., Kitzmann, C., Backhausen, J.E., and
835 Scheibe, R.** (2008). Knockout of major leaf ferredoxin reveals new redox-regulatory
836 adaptations in *Arabidopsis thaliana*. *Physiol. Plant.* **133**, 584-598.

837 **Waadt, R., Schmidt, L.K., Lohse, M., Hashimoto, K., Bock, R., and Kudla, J.** (2008).
838 Multicolor bimolecular fluorescence complementation reveals simultaneous formation of
839 alternative CBL/CIPK complexes *in planta*. *Plant J.* **56**, 505-516.

840 **Wang, Y.Q., Yang, Y., Fei, Z., Yuan, H., Fish, T., Thannhauser, T.W., Mazourek, M.,
841 Kochian, L.V., Wang, X., and Li, L.** (2013). Proteomic analysis of chromoplasts from six
842 crop species reveals insights into chromoplast function and development. *J. Exp. Bot.* **64**,
843 949-961.

844 **Waters, M.T., Moylan, E.C., and Langdale, J.A.** (2008). GLK transcription factors regulate
845 chloroplast development in a cell-autonomous manner. *Plant J.* **56**, 432-444.

846 **Welsch, R., Beyer, P., Hugueney, P., Kleinig, H., and von Lintig, J.** (2000). Regulation and
847 activation of phytoene synthase, a key enzyme in carotenoid biosynthesis, during
848 photomorphogenesis. *Planta* **211**, 846-854.

849 **Welsch, R., Wüst, F., Bär, C., Al-Babili, S., and Beyer, P.** (2008). A third phytoene synthase is
850 devoted to abiotic stress-induced abscisic acid formation in rice and defines functional
851 diversification of phytoene synthase genes. *Plant Physiol.* **147**, 367-380.

852 **Wurtzel, E.T., Cuttriss, A., and Vallabhaneni, R.** (2012). Maize provitamin a carotenoids,
853 current resources, and future metabolic engineering challenges. *Front. Plant Sci.* **3**, 29.

854 **Yang, Y., Zhang, S., Howe, K., Wilson, D.B., Moser, F., Irwin, D., and Thannhauser, T.W.**
855 (2007). A comparison of nLC-ESI-MS/MS and nLC-MALDI-MS/MS for GeLC-based
856 protein identification and iTRAQ-based shotgun quantitative proteomics. *J. Biomol. Tech.*
857 **18**, 226-237.

858 **Yuan, H., Zhang, J., Nageswaran, D., and Li, L.** (2015a). Carotenoid metabolism and
859 regulation in horticultural crops. *Hortic. Res.* **2**, 15036.

860 **Yuan, H., Owsiany, K., Sheeja, T.E., Zhou, X., Rodriguez, C., Li, Y., Welsch, R., Chayut, N.,
861 Yang, Y., Thannhauser, T.W., Parthasarathy, M.V., Xu, Q., Deng, X., Fei, Z., Schaffer,
862 A., Katzir, N., Burger, J., Tadmor, Y., and Li, L.** (2015b). A single amino acid substitution
863 in an ORANGE protein promotes carotenoid overaccumulation in *Arabidopsis*. *Plant Physiol.*
864 **169**, 421-431.

865 **Zhang, J., Yuan, H., Yang, Y., Fish, T., Lyi, S.M., Thannhauser, T.W., Zhang, L., and Li, L.**
 866 (2016). Plastid ribosomal protein S5 is involved in photosynthesis, plant development, and
 867 cold stress tolerance in *Arabidopsis*. *J. Exp. Bot.* **67**, 2731-2744.

868 **Zheng, B., Halperin, T., Hruskova-Heidingsfeldova, O., Adam, Z., Clarke, A.K. 2002.**
 869 Characterization of Chloroplast Clp proteins in *Arabidopsis*: Localization, tissue specificity
 870 and stress responses. *Physiol. Plant.* **114**, 92–101.

871 **Zhou, X., McQuinn, R., Fei, Z., Wolters, A.A., Van Eck, J., Brown, C., Giovannoni, J.J.,**
 872 **and Li, L.** (2011a). Regulatory control of high levels of carotenoid accumulation in potato
 873 tubers. *Plant Cell Environ.* **34**, 1020-1030.

874 **Zhou, X., Fei, Z., Thannhauser, T.W., and Li, L.** (2011b). Transcriptome analysis of ectopic
 875 chloroplast development in green curd cauliflower (*Brassica oleracea* L. var. *botrytis*). *BMC*
 876 *Plant Biol.* **11**, 169.

877 **Zhou, F., Wang, C-Y., Gutensohn, M., Jiang, L., Zhang, P., Zhang, D., Dudareva, N., Lu, S.**
 878 (2017). A recruiting protein of geranylgeranyl diphosphate synthase controls metabolic flux
 879 toward chlorophyll biosynthesis in rice. *Proc. Natl. Acad. Sci. USA* **114**, 6866–6871.

880 **Zhou, X., Welsch, R., Yang, Y., Álvarez, D., Riediger, M., Yuan, H., Fish, T., Liu, J.,**
 881 **Thannhauser, T.W., and Li, L.** (2015). *Arabidopsis* OR proteins are the major
 882 posttranscriptional regulators of phytoene synthase in controlling carotenoid biosynthesis.
 883 *Proc. Natl. Acad. Sci. USA* **112**, 3558-3563.

884 **Zybailov, B., Friso, G., Kim, J., Rudella, A., Rodríguez, V.R., Asakura, Y., Sun, Q., and van**
 885 **Wijk, K.J.** (2009). Large scale comparative proteomics of a chloroplast Clp protease mutant
 886 reveals folding stress, altered protein homeostasis, and feedback regulation of metabolism.
 887 *Mol. Cell Proteomics* **8**, 1789-1810.

888

889

890

891 **FIGURE LEGENTS**892 **Figure 1.** Interactions of PSY with Clp Subunits Involved in Substrate Selection.

893 **(A)** Interaction between PSY and ClpC1. Left: Y2H analysis. Interactions were examined by co-expressing pairs of proteins fused to either N-terminal or C-terminal ubiquitin moiety in yeast and spotting onto either nonselective (-LW) or fully selective medium plates with 300 μ M Met (-LWAH+M) in a series of 10-fold dilutions. Empty vectors expressing Nub and Cub only and a K⁺ channel protein (KAT1) were used as negative and unspecific controls, respectively. Right: BiFC analysis. PSY as C-terminal YFP fusion (YC) and ClpC1 as N-terminal fusion (YN) were co-expressed in *N. benthamiana* leaves. Empty vector expressing YC only was included as control.

901 **(B)** Interactions between PSY and Clp subunits. Left: Y2H analysis. Right: BiFC analysis of PSY interactions with ClpD, ClpC and ClpS1, as well as ClpS1 with ClpF or PRLI-interacting factor L (TAC).

904 **(C)** Interaction between PSY and HSP70. Left: Y2H analysis. Right: BiFC analysis.

905 Direct interactions in chloroplasts were observed by confocal microscopy (Scale bars, 20 μ m).
906 CHL, chlorophyll autofluorescence.

907

908 **Figure 2.** PSY Protein and Transcript Levels in the *clp* Mutants.909 **(A)** Representative images of 3-week-old *clp* mutants grown on soil.

910 **(B)** Immunoblot analysis of PSY protein levels. Actin was used as loading control. Analysis was
911 performed with 40 μ g leaf protein extracts from 3-week-old plants. Protein sizes (kD) are
912 indicated.

913 **(C)** Quantification of PSY protein levels normalized with actin. Results are means \pm SD from
914 quantification of three biological replicates.

915 **(D)** PSY mRNA levels determined by real-time RT-PCR. PSY transcripts were normalized to
916 *actin* levels and are expressed relative to one selected WT sample. Results are means \pm SD from
917 three biological replicates.

918 **(E)** PSY protein levels in *Arabidopsis* WT and unrelated chlorotic mutants (*rps5*, *xkl-1*, *toc33*,
919 *glk1/2*, and *fd2*) as well as the *hsp70-2* mutant. Actin was used as loading control.

920

921 **Figure 3.** PSY Protein Turnover Following Heat Treatment in *clpc1*.

922 (A) Immunoblot analysis of PSY turnover. The 3-week-old *Arabidopsis* WT and *clpc1* plants
 923 were transferred to 42°C. PSY protein levels in rosette leaves were determined before 0 min and
 924 after 15, 30 and 45 min of heat treatment. Ponceau S staining shows protein loading.
 925 (B) Relative PSY protein levels. PSY band intensities were normalized and expressed relative to
 926 the levels detected prior to heat treatment. Data represent the means \pm SD from three biological
 927 replicates.

928

929 **Figure 4.** Pigment Levels and Pathway Activity in the *clp* Mutants.

930 (A) Chlorophyll levels in the *clp* mutants.

931 (B) Carotenoid levels in the *clp* mutants. Pigments were determined from rosette leaves of 3-
 932 week-old plants by HPLC.

933 (C) Carotenoid/chlorophyll ratio from A and B.

934 (D) Carotenoid pathway activity was determined by illuminating 3-week-old leaves incubated
 935 with norflurazon for 4 h. Phytoene was quantified by HPLC and expressed relative to that
 936 determined in WT. Bleached leaf areas of *clpp4* were used for A, B and C while green leaves
 937 were used for D due to lack of materials. Results are means \pm SE from \geq three biological
 938 replicates. Significant difference, *P<0.05 in comparison with WT.

939

940 **Figure 5.** *In vitro* PSY Activity and Distribution in Chloroplasts of the *clp* Mutants.

941 (A) Western blot analysis of DXS, GGPS11, and PSY in chloroplast membrane and stroma
 942 fractions. RuBisCO large subunit (RbcL, stroma) and light harvesting complex of PSII subunit
 943 (Lhcb, membranes) protein levels from Coomassie-stained gels were used for protein loading
 944 controls.

945 (B) Absolute PSY activity in WT and *clp* mutants. Chloroplast membranes were incubated with
 946 supplemental GGPP synthase. Reactions were started with DMAPP and [1-¹⁴C]IPP. The
 947 synthesized product [1-¹⁴C]phytoene was quantified after 15 min of reaction.

948 (C) Total and specific PSY activity normalized to WT. Specific activity was normalized to the
 949 corresponding PSY protein levels determined in the WT or mutants (A).

950 Results are means \pm SD from three biological replicates. Significant difference, *P<0.05 in
 951 comparison with WT.

952

953 **Figure 6.** DXS and Other Carotenogenic Protein Levels in the *clp* Mutants.
 954 Immunoblot analysis of DXS and five addition carotenoid biosynthetic pathway enzymes. PDS:
 955 phytoene desaturase, ZDS: ζ -carotene desaturase, BCH: β -carotene hydroxylases, LUT5:
 956 carotenoid hydroxylase CYP97A3, and ZEP: zeaxanthin epoxidase. Analyses were performed
 957 with 20 μ g leaf protein extracts from 3-week-old plants of WT and the *clp* mutants. Membranes
 958 were stripped for reprobing 2-3 times. Actin signal from one representative blot is shown as
 959 loading control.

960

961 **Figure 7.** OR reduces PSY Turnover Rate and enhances PSY Activity in *clpc1*.
 962 (A) Representative immunoblot analysis of PSY-GFP fusion protein. PSY-GFP was expressed in
 963 WT (35S:PSY-GFP/WT) and in a line constitutively overexpressing *OR* (35S:PSY-GFP/OR).
 964 PSY protein stability was monitored by immunoblotting using an anti-GFP antibody prior (0 h)
 965 and at 3, 6 and 9 h following treatment with cycloheximide (CHX) to inhibit cytoplasmic protein
 966 translation. Ponceau S staining shows protein loading.
 967 (B) Relative PSY protein levels. PSY band intensities were quantified and expressed relative to
 968 the levels detected prior to CHX treatment. Results are means \pm SD from quantification of three
 969 biological replicates.
 970 (C) Immunoblot analysis of OR protein levels. Actin level is shown as loading control.
 971 (D) Phytoene accumulation in leaves of 3-week-old plants following treatment with norflurazon
 972 for 4 h. Phytoene in *clpc1*, *AtOR*-overexpressing line (*OR*) and double homozygous crossing
 973 (*clpc1* x *OR*) was quantified by HPLC and expressed relative to that determined in WT. Results
 974 are means \pm SD from three biological replicates. Phytoene amounts from all lines/WT were
 975 significantly different from each other (student's *t*-test, *P<0.05).

976

977 **Figure 8.** Model on Counterbalance of PSY Proteostasis by Clp Protease and OR.
 978 Membrane-associated PSY requires interaction with the membrane-integral holdase OR in order
 979 to remain properly folded and enzymatically active. Misfolded PSY is recognized by Clp adaptor
 980 proteins and gets degraded by the Clp protease system through direct protein-protein interactions.
 981 OR maintains the population of properly folded PSY proteins and thus carotenogenesis, while
 982 absence of OR results in PSY degradation. Deficiency in Clp activity reduces PSY proteolysis
 983 and results in the accumulation of PSY populations, which contained enzymatically inactive as

984 well as active forms probably due to increased chaperone proteins to help folding or prevent
985 aggregations.

986

987

988 **SUPPLEMENTAL INFORMATION**

989 The following materials are available in the online version of this article:

990 **Supplemental Figure 1.** Two independent transgenic lines expressing *35S:PSY-GFP*

991 **Supplemental Figure 2.** Negative controls for interaction studies

992 **Supplemental Figure 3.** Generation of *clpp4* Antisense lines

993 **Supplemental Figure 4.** Carotenoid levels in *clp* mutants after NFZ treatment

994 **Supplemental Figure 5.** GGPS activity in chloroplast membrane fractions

995 **Supplemental Figure 6.** PSY-GFP fusion protein expression in WT and *OR*-overexpression
996 background

997 **Supplemental Figure 7.** Interaction between ClpS1 and mature PSY N-terminal sequence
998 containing a putative N-degron by Y2H

999 **Supplemental Figure 8.** Interaction between Hsp70, PSY and OR by Y2H assays

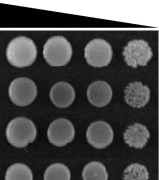
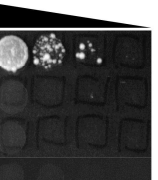
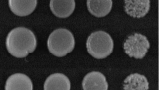
1000 **Supplemental Figure 9.** Hsp70 and Hsp90 Levels in the *clp* mutants

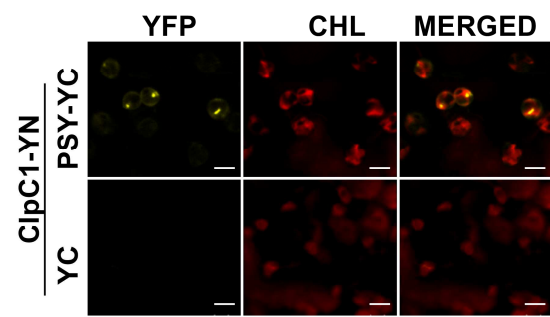
1001 **Supplemental Table 1.** Proteins identified in *35S:PSY-GFP* and *35S:GFP* *Arabidopsis* plants by
1002 co-IP and MS

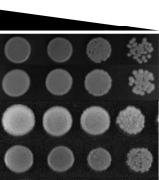
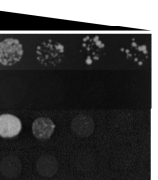
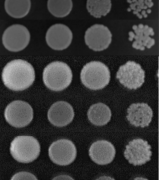
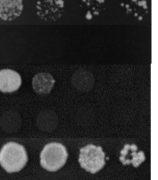
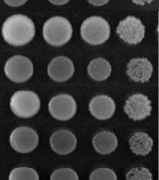
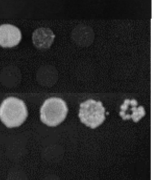
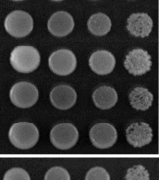
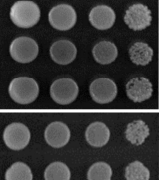
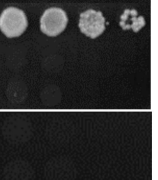
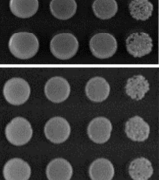
1003 **Supplemental Table 2.** Common proteins in quadruplicate PSY-GFP samples but absent in the
1004 GFP only controls

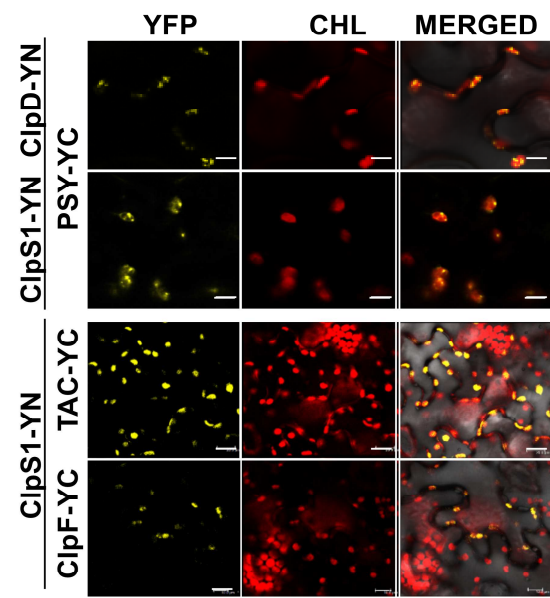
1005 **Supplemental Table 3.** List of primers used in this study

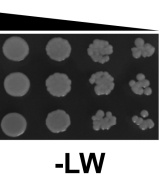
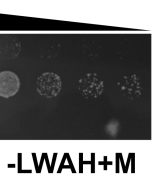
A

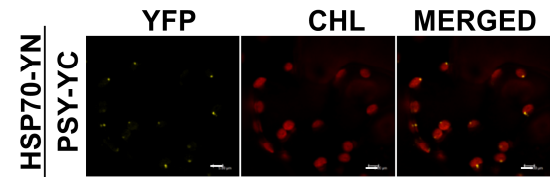
<u>Nub</u>	<u>Cub</u>	
ClpC1	PSY	
ClpC1	Cub	
Nub	PSY	
ClpC1	KAT1	
		-LW -LWAH+M

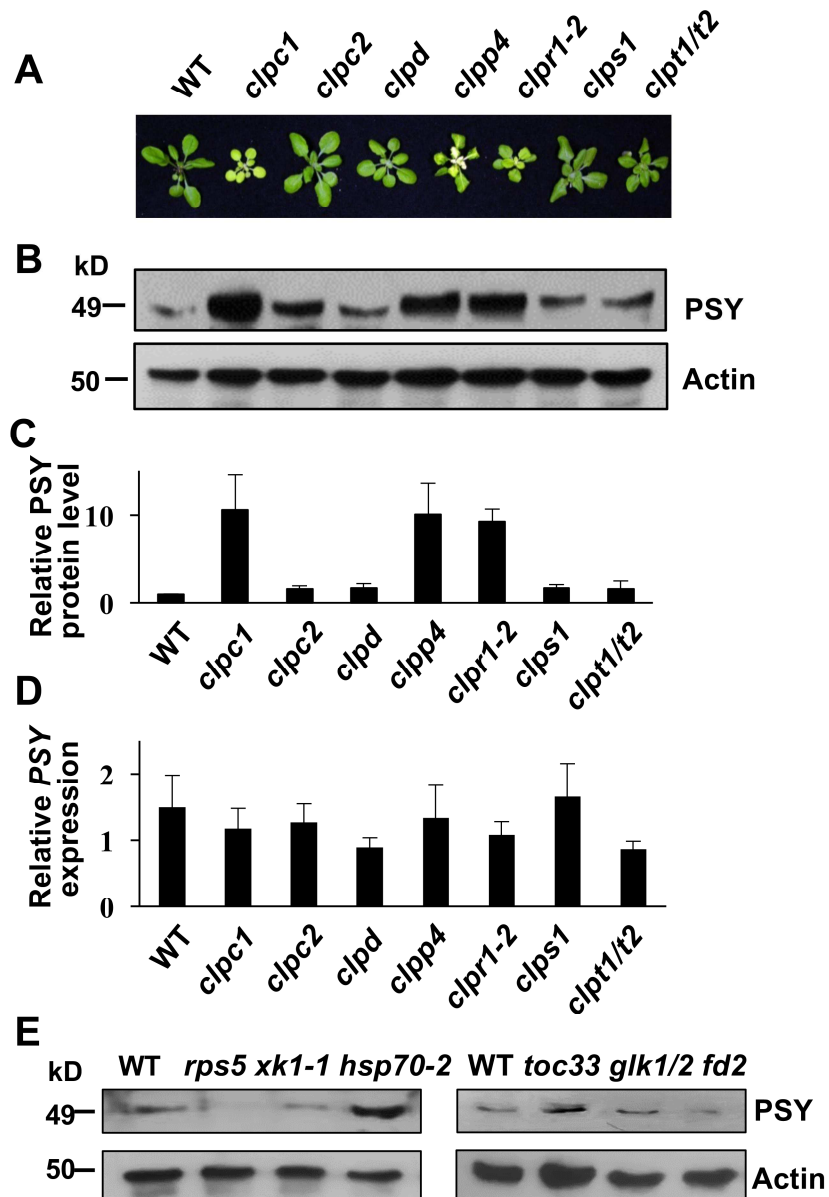
**B**

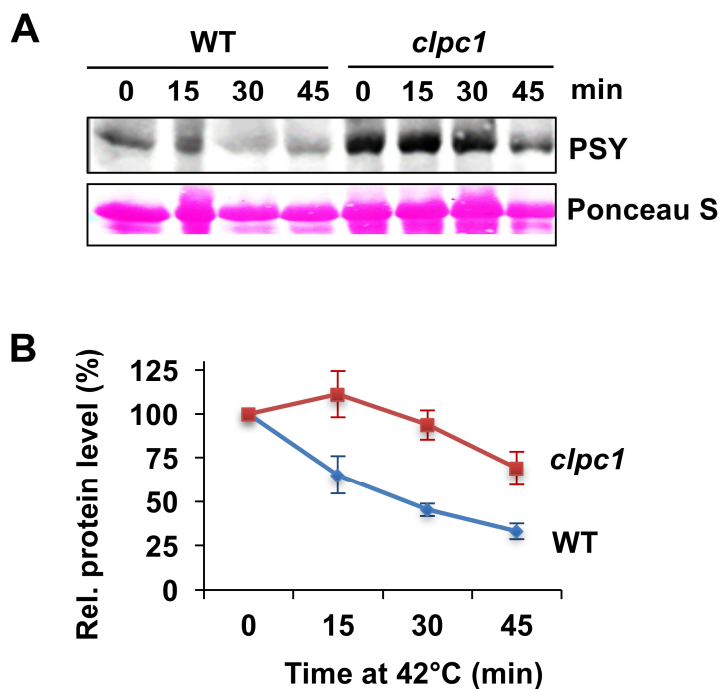
<u>Nub</u>	<u>Cub</u>	
ClpD	PSY	
ClpD	Cub	
ClpC2	PSY	
ClpC2	Cub	
ClpS1	PSY	
ClpS1	Cub	
Nub	PSY	
ClpC2	KAT1	
ClpS1	KAT1	
Nub	KAT1	
		-LW -LWAH+M

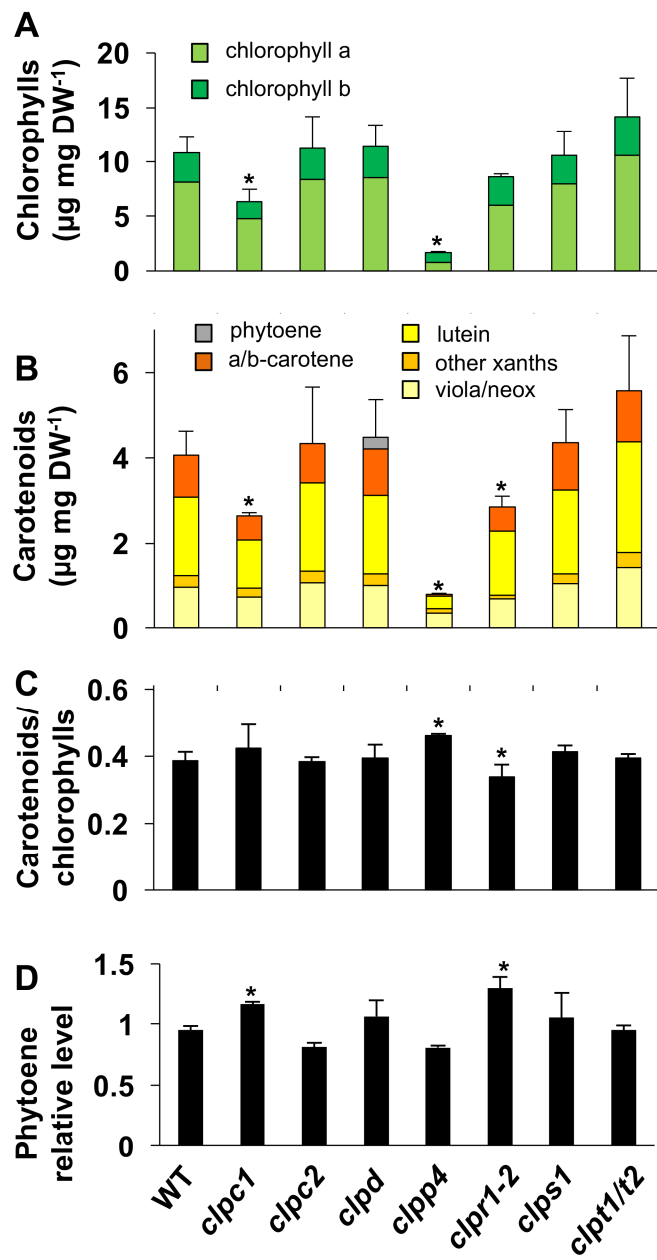
**C**

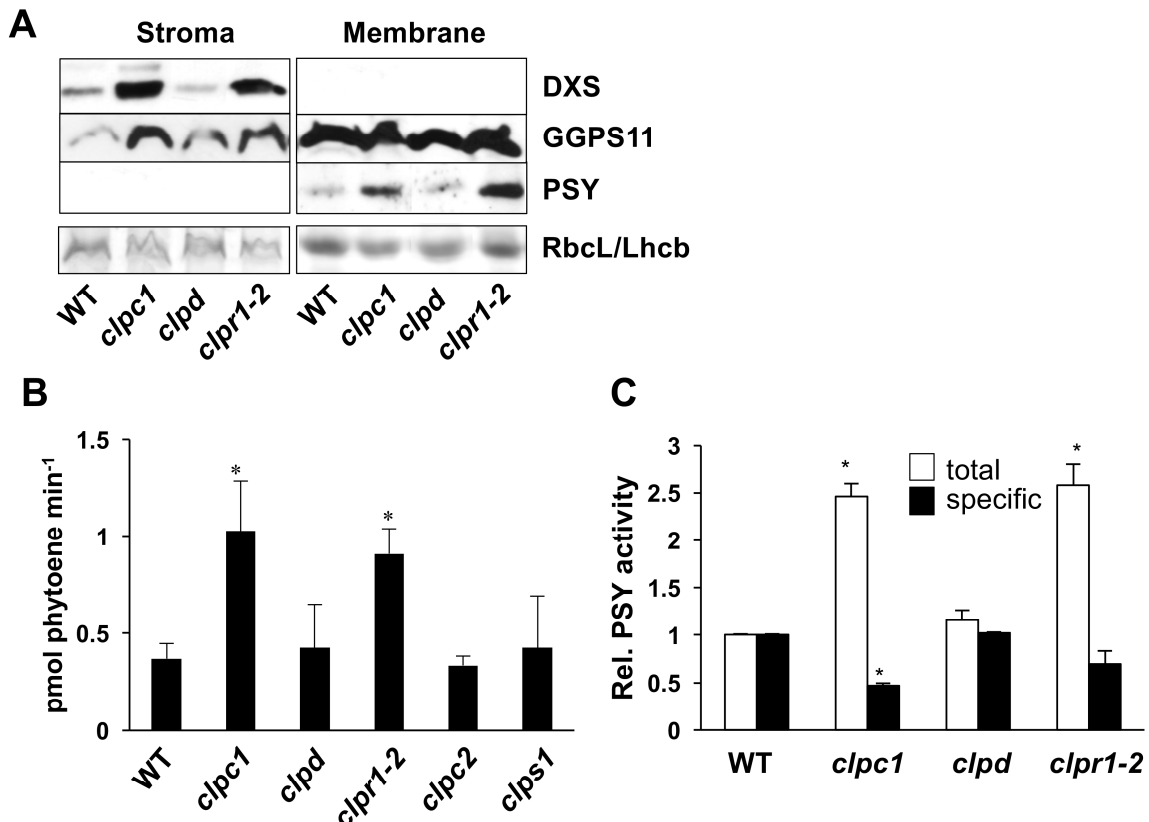
<u>Nub</u>	<u>Cub</u>	
Nub	PSY	
HSP70	PSY	
HSP70	Cub	
		-LW -LWAH+M

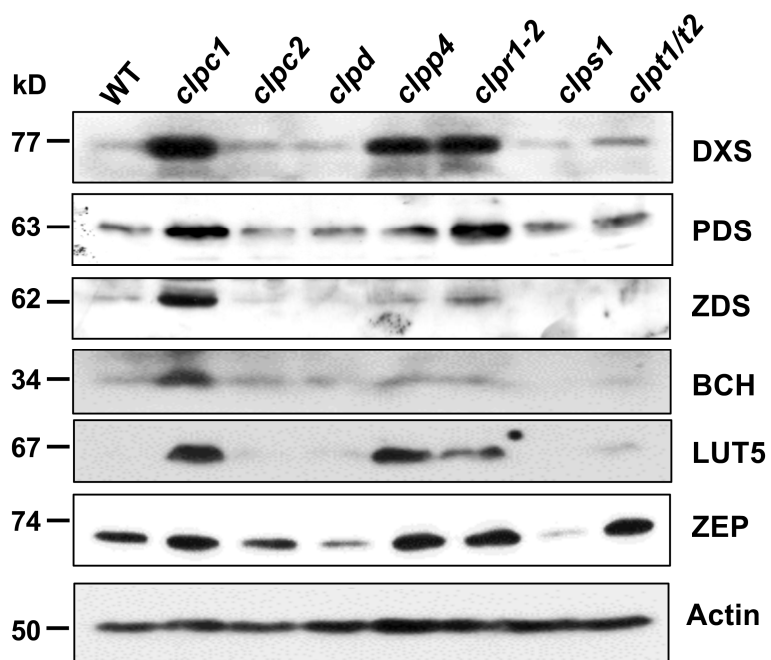


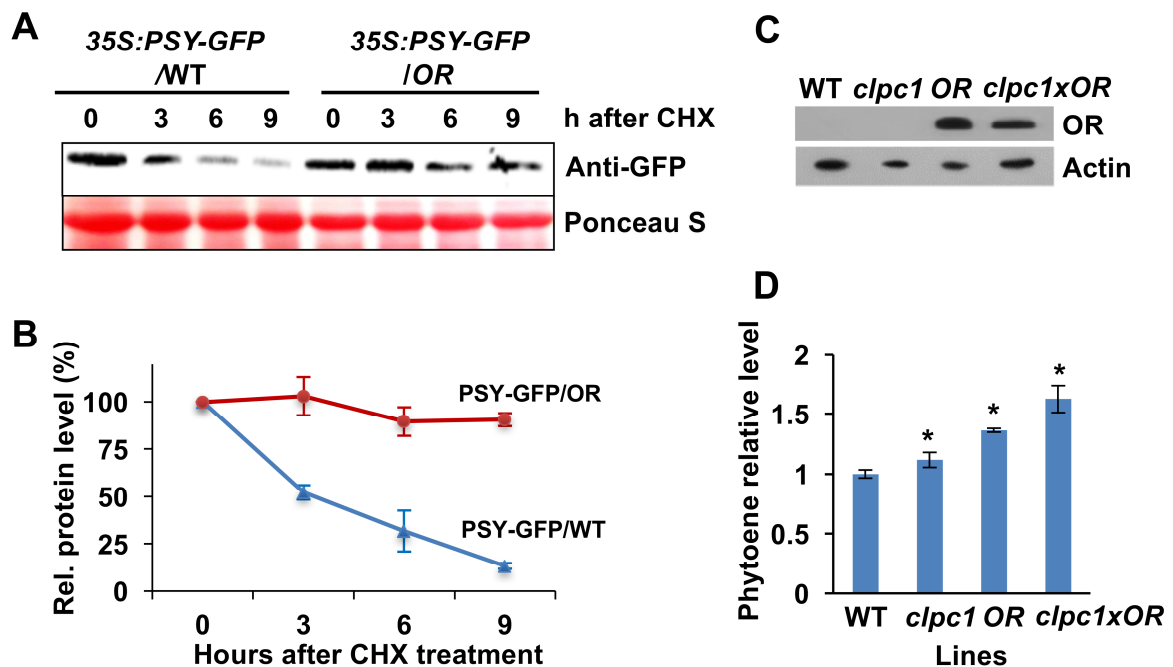


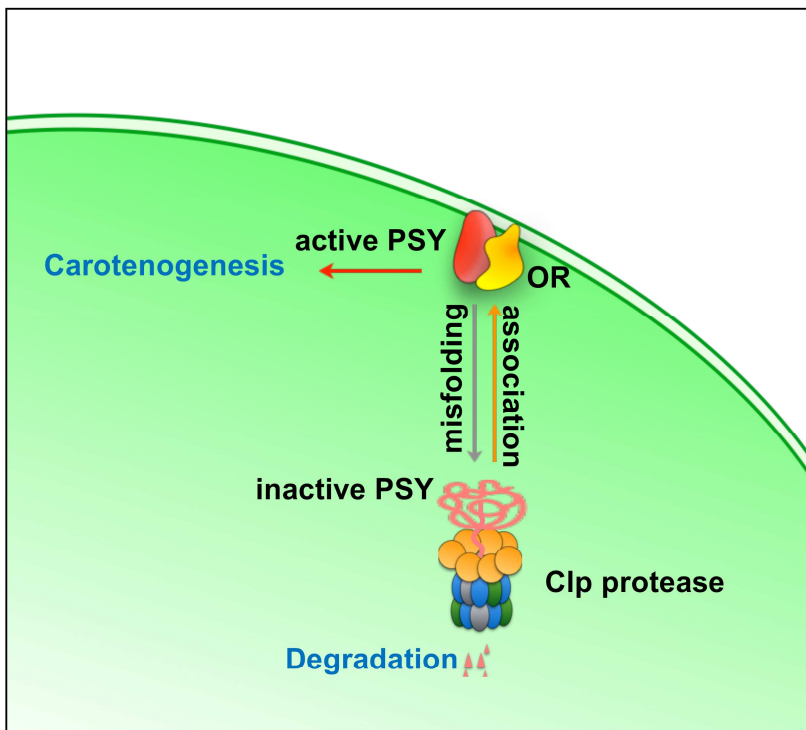


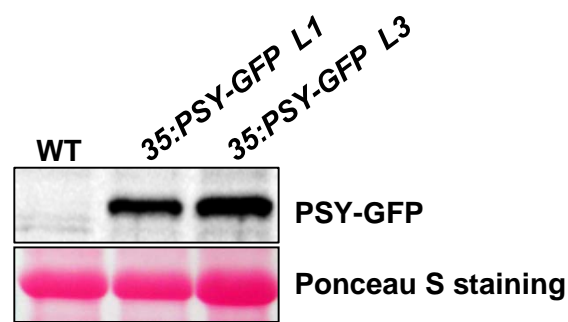




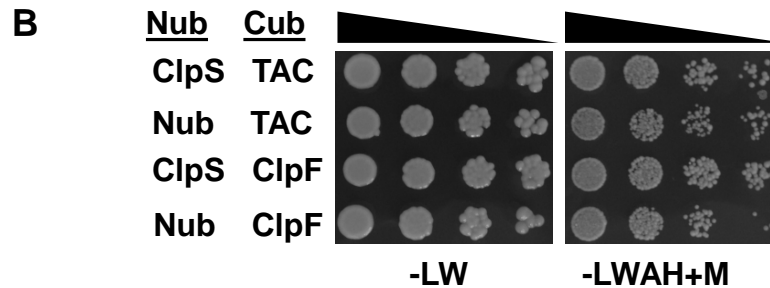
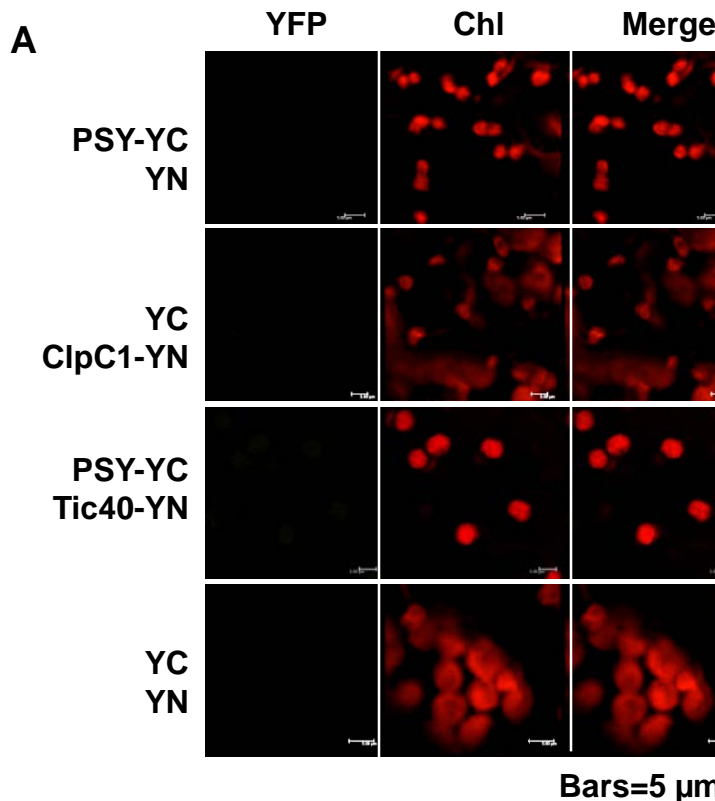








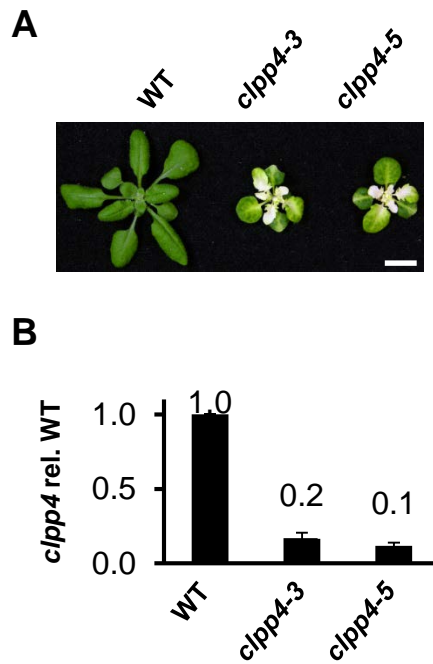
Supplemental Figure 1. Two independent transgenic lines expressing *35S:PSY-GFP*. Ponceau S staining shows protein loading.



Supplemental Figure 2. Negative Controls for Interaction Studies.

(A) BiFC negative controls for PSY and ClpC1 interaction. PSY-YC, ClpC1-YN were co-expressed with the corresponding N- or C-terminal YFP (YN and YC, respectively) in *N. benthamiana* leaves. In addition, PSY-YN was coexpressed with Tic40-YN as unspecific negative control and empty vector control (YC+YC). No interactions were found in chloroplasts. Bars = 5 μ m, CHL, chlorophyll autofluorescence.

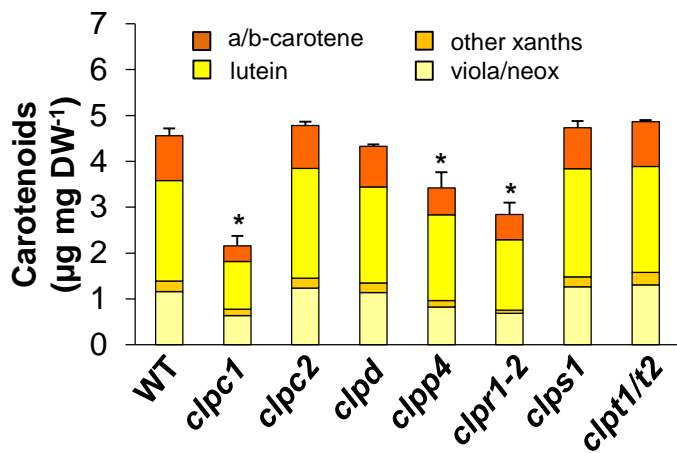
(B) Y2H analysis with PRL1-interacting factor L (TAC) and ClpF. Interactions were examined by coexpression of pairs of proteins fused to either N-terminal or C-terminal ubiquitin moiety in yeast and spotted onto either nonselective (-LW) or fully selective medium plates (supplemented with 1 mM Met; -LWAH+M) in a series of 10-fold dilutions. Expression of TAC and ClpF showed strong reporter gene autoactivation, indicated by yeast growth in presence of only empty vectors expressing Nub and Cub. Therefore, specific interactions between ClpSa/TAC and ClpS1/ClpF could not be analyzed with this system.



Supplemental Figure 3. Generation of *clpp4* Antisense Lines.

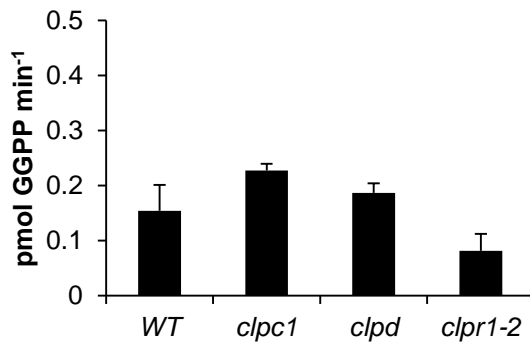
(A) *Clpp4* antisense construct was constitutively expressed in *Arabidopsis* WT (Col-0). Representative pictures from 4-week-old WT and two selected *clpp4* antisense lines. Bar = 1 cm.

(B) *ClpP4* expression levels were determined by real-time RT-PCR, normalized to actin levels and expressed relative to WT levels.



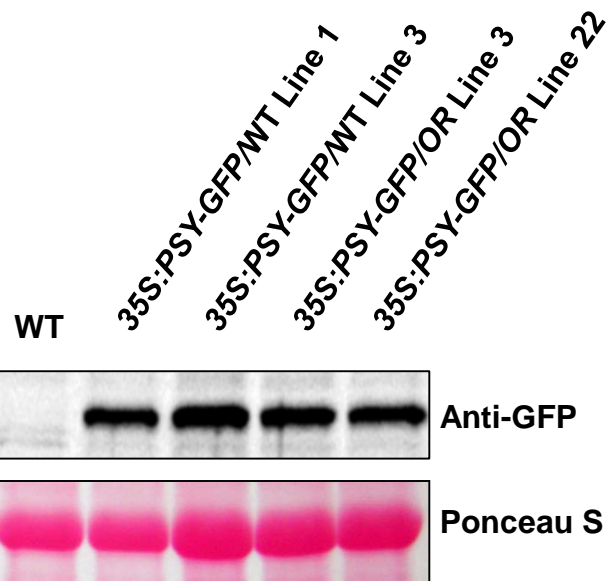
Supplemental Figure 4. Carotenoid Levels in the *clp* Mutants after NFZ Treatment.

Carotenoid levels were determined in 3-week-old leaves incubated with norflurazon for 4 h. Phytoene levels are not shown. Results are means \pm SE from \geq three biological replicates. Significant difference, *P<0.05 in comparison with WT.



Supplemental Figure 5. GGPS Activity in Chloroplast Membrane Fractions.

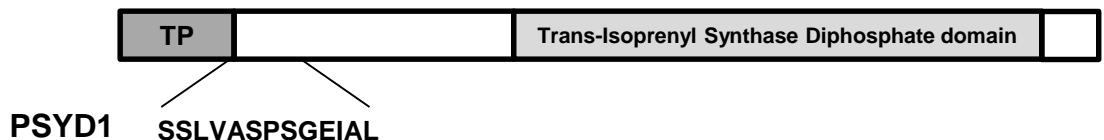
Chloroplast membranes from 3-week-old plants were incubated with DMAPP and [1-¹⁴C]IPP. The synthesized product [1-¹⁴C]GGPP was quantified. No significant differences (student's *t*-test, $P < 0.05$) were determined for the mutant lines in comparison with wild-type control. Data are mean of two biological replicates.



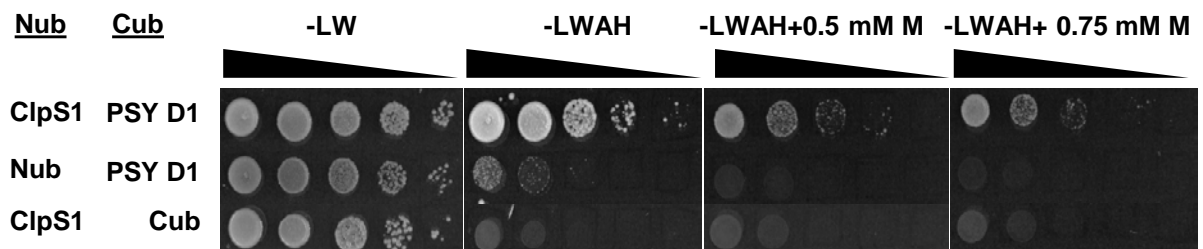
Supplemental Figure 6. PSY-GFP Fusion Protein Expression in WT and *OR* Overexpression Background.

PSY-GFP was constitutively expressed in WT (35S:PSY-GFP/WT lines 1 and 3) and in a transgenic line overexpressing *AtOR* (35S:PSY-GFP/OR lines 3 and 22). Immunoblot analysis of leaf protein extracts using anti-GFP antibodies. Two lines with similar level of PSY-GFP protein expression were used for PSY stability experiments in Figure 7.

A



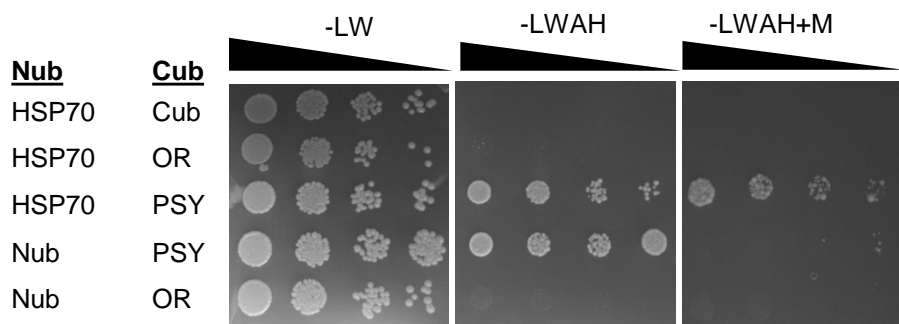
B



Supplemental Figure 7. Interaction Between ClpS1 and Mature PSY N-terminal Sequence Containing a Putative N-Degron by Y2H.

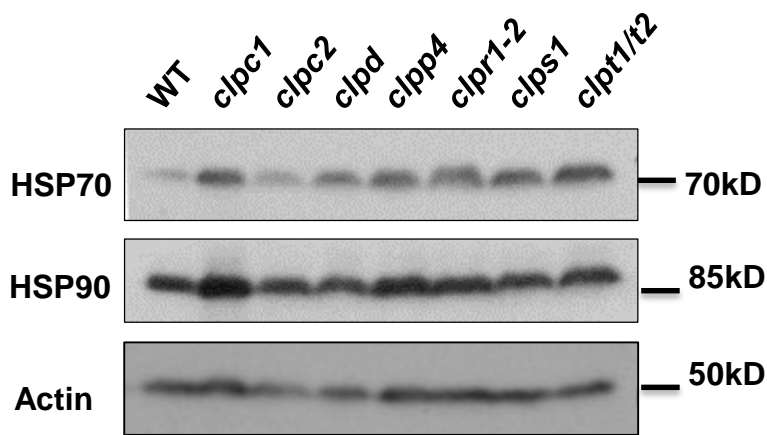
(A) PSY protein structure. PSYD1 contains 13 amino acids (#71-83) as indicated.

(B) Y2H analysis. ClpS1 interacts with PSYD1 fragment in yeast.



Supplemental Figure 8. Interactions Between Hsp70, PSY and OR by Y2H Assay.

Interactions were examined by coexpression of pairs of proteins fused to either N-terminal or C-terminal ubiquitin moiety in yeast and spotted onto either nonselective (-LW) or fully selective medium plates (supplemented with 150 μ M Met; -LWAH+M) in a series of 10-fold dilutions. Empty vectors expressing Nub and Cub only were used as negative or unspecific controls, respectively.



Supplemental Figure 9. Hsp70 and Hsp90 Levels in the *clp* Mutants.

Immunoblot analyses were performed with 80 μ g leaf protein extracts from 3-week-old plants of WT and the *clp* mutants. Membranes were stripped for reprobing. Actin is shown as loading control.